© 2016. Published by The Company of Biologists Ltd | Journal of Cell Science (2016) 129, 2416-2429 doi:10.1242/jcs.184721

RESEARCH ARTICLE

Cortactin is a scaffolding platform for the E-cadherin adhesion complex and is regulated by protein kinase D1 phosphorylation

Robert Sroka[1], Johan Van Lint[2], Sarah-Fee Katz[1], Marlon R. Schneider[3], Alexander Kleger[1], Stephan Paschke[4], Thomas Seufferlein[1] and Tim Eiseler[1,*]

ABSTRACT

Dynamic regulation of cell–cell adhesion by the coordinated formation and dissolution of E-cadherin-based adherens junctions is crucial for tissue homeostasis. The actin-binding protein cortactin interacts with E-cadherin and enables F-actin accumulation at adherens junctions. Here, we were interested to study the broader functional interactions of cortactin in adhesion complexes. In line with literature, we demonstrate that cortactin binds to E-cadherin, and that a posttranslational modification of cortactin, RhoA-induced phosphorylation by protein kinase D1 (PKD1; also known as PRKD1) at S298, impairs adherens junction assembly and supports their dissolution. Two new S298-phosphorylation-dependent interactions were also identified, namely, that phosphorylation of cortactin decreases its interaction with β-catenin and the actin-binding protein vinculin. In addition, binding of vinculin to β-catenin, as well as linkage of vinculin to F-actin, are also significantly compromised upon phosphorylation of cortactin. Accordingly, we found that regulation of cell–cell adhesion by phosphorylation of cortactin downstream of RhoA and PKD1 is vitally dependent on vinculin-mediated protein interactions. Thus, cortactin, unexpectedly, is an important integration node for the dynamic regulation of protein complexes during breakdown and formation of adherens junctions.

KEY WORDS: Cortactin, Adherens junction, Vinculin, Protein kinase D, PKD, Cadherin-1, CDH1, Epithelial cadherin, E-cadherin

INTRODUCTION

Epithelial cells are tightly interconnected and form two-dimensional multicellular sheets (Takeichi, 2014). In vertebrates, cell–cell adhesion is mediated by specialized structures: tight junctions, adherens junctions and desmosomes (Takeichi, 2011). Adherens junctions are present in all tissue-forming cells and constitute cell junctions that are linked to the actin cytoskeleton at their cytoplasmic side. They are dynamic structures that regulate cell shape, maintain tissue integrity and translate acto-myosin-generated forces throughout a tissue. They also play a major role in embryonic morphogenesis, as well as the formation and homeostasis of epithelial tissues (Schneider and Kolligs, 2015; Takeichi, 2011). Adherens junctions are formed by the recruitment of transmembrane cadherins, catenins and cytoskeletal adaptor proteins. The prototype cadherin in epithelial cells is E-cadherin. Upon homophilic interaction of its extracellular domains, the intracellular domain of E-cadherin associates with cytoplasmic proteins, such as catenins, that provide a link to the actin cytoskeleton and dynamically regulate adhesion strength (Aberle et al., 1996; Davis et al., 2003; Hartsock and Nelson, 2008; Huber and Weis, 2001; Ireton et al., 2002; Rimm et al., 1995; Rimm and Morrow, 1994). The juxtamembrane portion of the E-cadherin cytoplasmic domain associates with p120-catenin (also known as CTNND1), whereas its C-terminal part binds to β-catenin or plakoglobin (Shibamoto et al., 1994; Takeichi et al., 1994). β-Catenin has been suggested to interact with α-catenin, which harbors an F-actin-binding motif (Provost and Rimm, 1999). Drees et al. (2005a) and Yamada et al. (2005) have demonstrated that *in vitro* monomeric α-catenin in a complex with E-cadherin and β-catenin is unable to bind F-actin (Benjamin et al., 2010; Drees et al., 2005a; Pokutta et al., 2008; Weis and Nelson, 2006; Yamada et al., 2005). Recent data suggest that the stable binding of this complex to F-actin *in vitro* requires mechanical force (Buckley et al., 2014). It is as yet unclear how a short-lived, weak binding in the absence of force is transformed into a force-dependent, stable interaction *in vivo*. Thus, other actin-binding and putative scaffolding proteins might be part of this dynamic process. One of these factors is the actin-binding protein vinculin. This protein has been demonstrated to bind to α-catenin under force, linking the adhesion complex to F-actin (Yonemura et al., 2010). The actin-regulatory protein cortactin is also an important part of the adhesion complex and directly binds to E-cadherin (Helwani et al., 2004). Cortactin is required for the E-cadherin–actin cooperation and actin accumulation that supports the formation of adherens junctions (Helwani et al., 2004).

Our previous data have shown that cortactin is phosphorylated at S298 by protein kinase D1 (PKD1; also known as PRKD1) and this results in 14-3-3 protein binding (Eiseler et al., 2010). 14-3-3-phospho-motif-binding proteins are known for their ability to modulate protein interactions following phosphorylation of consensus motifs (Aitken, 2006; Mackintosh, 2004). PKD proteins have also been implicated in cell–cell adhesion, but the precise molecular mechanisms are as yet elusive (Janssens et al., 2009; Sundram et al., 2012). Here, we aimed to further elucidate the role of cortactin and its posttranslational modification by PKD1 during the dynamic processes associated with the formation or dissolution of adherens junctions.

RESULTS

Cortactin and PKD1 regulate cell–cell adhesion in a similar manner

Previous work has described an interaction between cortactin and E-cadherin in adherens junctions, and a role for cortactin in actin accumulation at adherens junctions during contact zone extension

[1]Department of Internal Medicine I, Ulm University, Albert-Einstein-Allee 23, Ulm 89081, Germany. [2]Department of Cellular and Molecular Medicine, Katholieke Universiteit Leuven, Campus Gasthuisberg O/N1 - Herestraat 49 bus 901, Leuven 3000, Belgium. [3]Department for Animal Breeding and Biotechnology, LMU Munich, Gene Center, Feodor-Lynen-Str. 25, Munich 81377, Germany. [4]Department of Visceral Surgery, Ulm University, Albert-Einstein-Allee 23, Ulm 89081, Germany.

*Author for correspondence (tim.eiseler@uniklinik-ulm.de)

T.E., 0000-0001-7819-4659

Received 10 December 2015; Accepted 28 April 2016

Journal of Cell Science (2016) 129, 2416-2429 doi:10.1242/jcs.184721

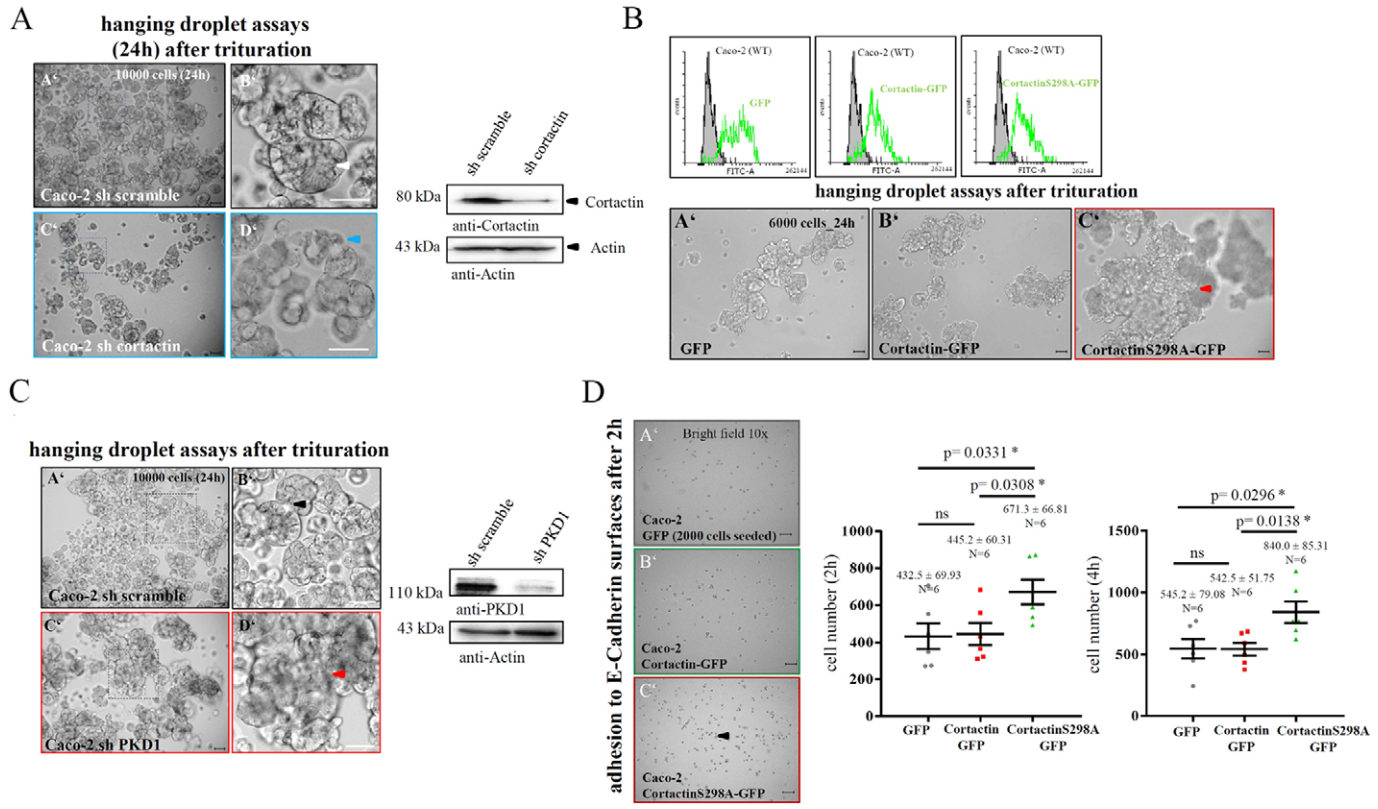

Fig. 1. Cortactin and its phosphorylation by PKD1 modulate E-cadherin-mediated cell–cell adhesion. (A) Hanging droplet cell–cell adhesion assays with Caco-2 cells following stable knockdown of cortactin (sh cortactin). Panels A′–D′ show representative images of three independent experiments, six replica droplets per condition. 10,000 cells per 20 µl were incubated in hanging droplets for 24 h followed by trituration. Images taken at 10× magnification and magnifications of rectangle regions of interest are shown. sh scramble, scrambled control shRNA. Scale bars: 100 µm. The western blot shows cortactin knockdown in cell lysates. (B) Panels A′–C′ show hanging droplet assays of stable polyclonal Caco-2 cells expressing GFP, cortactin–GFP and cortactin-S298A–GFP. Expression was analyzed by flow cytometry (histograms at the top). Assays were performed from three independent sources, six replica droplets per condition (6000 cells per 20 µl). Representative images are shown. Scale bars: 100 µm. (C) Panels A′–D′ show hanging droplet assays with stable Caco-2 cells following PKD1 depletion (sh PKD1). Experiments were performed as described in A with 10,000 cells per 20 µl droplet. Scale bars: 100 µm. The western blot shows knockdown of PKD1 in cell lysates. (D) Cell adhesion assays of stable Caco-2 cells expressing GFP, cortactin–GFP and cortactin-S298A–GFP (as characterized in B) on E-cadherin-bio-functionalized glass surfaces. 2000 cells per 20 µl droplets (two replicas per condition and three experiments) were incubated for 2 and 4 h. Panels A′–C′ show a random area taken at 10× magnification after 2 h. Scale bars: 100 µm. The left-hand graph shows the mean±s.e.m. number of adhered cells; the right-hand graph shows the mean±s.e.m. number of adhered cells after 4 h. *P<0.05; ns, not significant (two-tailed unpaired Student's t-test). Colored arrowheads mark clusters.

(Helwani et al., 2004; Ren et al., 2009). Our experiments therefore aimed at investigating the role of cortactin in E-cadherin-mediated cell–cell adhesion. To assess cortactin-dependent changes in cell–cell adhesion, we performed hanging droplet trituration assays, where adhesion is determined by evaluating the size and cohesion of cell aggregates following extensive resuspension (Bardella et al., 2004; Lorch et al., 2004). Our data showed that stable knockdown of cortactin in Caco-2 cells visibly impaired cell–cell adhesion after 24 h (Fig. 1A). We have previously described a posttranslational modification of cortactin by PKD1 resulting in phosphorylation of cortactin at S298. As a consequence, 14-3-3 proteins bind to the phosphorylated consensus motif and alter protein function (Eiseler et al., 2010). PKD1 activity in turn is controlled by the GTPase RhoA (Eiseler et al., 2009), which is also involved in signaling pathways modulating adherens junctions. We therefore examined whether PKD1 and cortactin act in a common pathway controlling cell–cell adhesion. We performed hanging droplet trituration assays using polyclonal stable Caco-2 cells expressing GFP-vector, cortactin- and the non-phosphorylatable cortactin-S298A–GFP mutant (Fig. 1B). The clusters formed in the presence of wild-type cortactin were small and did not substantially differ from controls, whereas S298A-cortactin mutant cells displayed markedly bigger clusters, indicating enhanced cell–cell adhesion (Fig. 1B). In parallel, we examined the effect of a stable short hairpin RNA (shRNA)-mediated PKD1 depletion (Fig. 1C). Knockdown of PKD1 also enhanced cell–cell adhesion in accordance with the cortactin-S298A mutant phenotype. Given that binding of 14-3-3 proteins to phospho-consensus motifs is dependent on the presence of a phosphate residue and not only on a negative charge (Ferl et al., 2002; Mackintosh, 2004), we were not able to additionally employ phosphorylation-mimicking mutations of cortactin in our experiments. Cell–cell adhesion was further assessed using constitutively active (PKD1-CA) and dominant-negative, kinase-inactive (PKD1-KD) forms of PKD1 (Fig. S1A). Active PKD1 visibly impaired cell–cell adhesion with or without co-expression of cortactin, whereas kinase-inactive PKD1-KD strongly enhanced cell aggregation in accordance with the PKD1-knockout phenotype (Fig. S1A). Actin accumulation and F-actin binding of cortactin are important features that determine the role of cortactin at adherens junctions (Han et al., 2014). To evaluate PKD1-mediated cell–cell adhesion phenotypes in the context of these factors, we also performed aggregation assays using a cortactin-W22A mutant,

Journal of Cell Science (2016) 129, 2416-2429 doi:10.1242/jcs.184721

abrogating Arp3 interaction, as well as a cortactin-6A mutant that was generated to impair F-actin binding by alanine point mutations in the actin-binding repeats 1, 4 and 6 (see Fig. S1B). Both mutations visibly impaired cell–cell adhesion resulting in phenotypes comparable to the PKD1-CA or PKD1-CA with cortactin samples. Rescue experiments upon stable depletion of cortactin and re-expression of shRNA-resistant cortactin or cortactin-S298A constructs further indicated that wild-type cortactin was able to rescue cell–cell adhesion in cortactin-depleted cells. In contrast, expression of cortactin-S298A enhanced cell–cell adhesion similar to the overexpression phenotypes (Fig. S1C,D). Our data therefore suggest a robust regulation of cell–cell adhesion by phosphorylation of cortactin at S298 mediated by PKD1.

In order to quantify the extent of cell–cell adhesion for single cells, we employed bio-functionalized glass surfaces presenting purified extracellular E-cadherin–Fc fragments (Fig. 1D) (Drees et al., 2005b) to measure adhesion of the stable cortactin-expressing cell lines. Cells were seeded in droplets on these glass slides and incubated for 2 or 4 h (Fig. 1D). We then quantified the number of cells adhered to the surface of the droplet area. In line with hanging droplet assays, there was no difference in the number of adherent cells between wild-type cortactin or the control samples, whereas the number of adherent cells significantly increased for the cortactin-S298A mutant, corresponding to increased adhesion at the E-cadherin-modified surface (Fig. 1D).

To identify a putative function of PKD1 during the formation or dissolution of adherens junctions, we incubated confluent Caco-2 cells transiently expressing PKD1-CA or PKD1-KD in patches with EGTA for 10 min and performed reformation kinetics by re-adding Ca^{2+}. During forced dissolution of adherens junctions by Ca^{2+} depletion up to the 10-min time point we were not able to identify differences at adherens junctions, indicated by E-cadherin staining, for the respective conditions (data not shown). Expression of active PKD1-CA did not further enhance adherens junction breakdown on top of EGTA treatment and expression of PKD1-KD did not counteract forced dissolution of adherens junctions after impairment of E-cadherin function, in line with the loss of cortactin–E-cadherin complexes when adherens junctions are dissolved. However, during formation of adherens junctions, presence of inactive PKD1-KD strongly increased E-cadherin signals at adherens junctions after 20 (Fig. S1E, panels I′,J′) and 60 min (Fig. S1E, panels M′,N′), whereas junctional E-cadherin staining was not as prominent for PKD1-CA cells (Fig. S1E). Thus, inactive PKD1 or impaired phosphorylation of cortactin at S298 seems to foster E-cadherin-mediated adherens junction assembly and intercellular adhesion.

PKD1 is activated by adherens junction breakdown and inactivated during assembly

We therefore investigated next, whether PKD1 and cortactin would interact at adherens junctions using acceptor-photobleach fluorescence resonance energy transfer (AB-FRET, Fig. 2A). This method allows us to study direct protein interactions in fixed samples. If FRET donors and acceptors reside within distances <10 nm, non-radiative energy transfer from a donor to an acceptor can occur, impairing donor fluorescence intensity. FRET is quantified by measuring the increase in donor intensity upon acceptor depletion (Fig. 2A). AB-FRET analysis indicated that endogenous PKD1 interacted with cortactin–GFP and, vice versa, that PKD1–GFP interacted with endogenous cortactin at Caco-2 adherens junctions. FRET studies with the adhesion-resident Afadin protein were used as negative control (Fig. 2B; Fig. S2A). These data suggest that PKD1 is physically able to phosphorylate cortactin at adherens junctions. If this was indeed the case, PKD1 might be inactivated during adherens junction assembly and activated upon breakdown of adherens junctions. To examine the activation state of PKD1 and its phosphorylation of cortactin during adherens junction disassembly, we performed Ca^{2+}-quenching experiments in Caco-2 cells. PKD1 was activated after addition of EGTA to medium as indicated by an increase in S910 auto-phosphorylation, and PKD1 activation also resulted in corresponding phosphorylation of cortactin at S298 (Fig. 2C). To verify PKD1 activation in response to adherens junction dissolution, we also quantified S910 phosphorylation after addition of E-cadherin-blocking antibodies (DECMA-1). Again, PKD1 was significantly activated upon dissolution of adherens junctions by DECMA treatment (Fig. 2D,E). To assess PKD1 activation kinetics, we subsequently performed Ca^{2+}-quenching experiments. PKD1 was significantly activated by addition of EGTA for 30 s (Fig. 2F,G) and re-ligation of cell–cell adhesions significantly decreased PKD1 activity (Fig. 2G). PKD1 auto-phosphorylation even dropped below basal levels after 5, 10 and 20 min of reformation for the displayed signal (Fig. 2F). Thus, PKD1 activity was impaired during adherens junction formation and enhanced when adherens junctions were dissolved. To quantify the corresponding phosphorylation of cortactin at S298 in response to EGTA treatment, we detected anti-phospho-S298-antibody signals at adherens junctions of Caco-2 cells. In line with the PKD1 activation kinetics, pS298-cortactin levels at adherens junctions significantly increased after 1 and 2 min of EGTA stimulation. After 2 min, signals started to significantly decrease and were almost completely lost at the 5-min time point, where adherens junction integrity was also visibly affected by Ca^{2+} depletion (see arrowhead, Fig. S2B,C).

PKDs, and especially PKD1, are activated downstream of active RhoA (Eiseler et al., 2009) (Fig. S2D,E). During ligation of E-cadherin-based cell–cell adhesions, RhoA is inhibited by recruitment of p190RhoGAP-A (also known as ARHGAP35) (Noren et al., 2003; Wildenberg et al., 2006). Indeed, using a RhoA FRET biosensor (Pertz et al., 2006), we show that RhoA activity is regulated by dissolution and re-formation of adherens junctions: dissolution of Caco-2 adherens junctions by EGTA activated RhoA, whereas reformation of adherens junctions utilizing $CaCl_2$ impaired RhoA activity (Fig. 2H). A control for biosensor specificity during EGTA-triggered activation of RhoA is shown is Fig. S2F utilizing an inactive RhoA-T19N-sensor derivate.

In agreement with RhoA activation experiments, hanging-droplet assays with inactive RhoA-T19N and p190RhoGAP-A displayed enhanced cell aggregation, whereas the GTP-locked constitutively active RhoA-V14 variant reduced aggregate size as compared to controls (Fig. S2G).

To evaluate the role of p190RhoGAP-A and RhoA in the regulation of PKD1 during disassembly and re-formation of adherens junctions, we assessed Ca^{2+}-quenching kinetics. Activation of RhoA by Ca^{2+}-quenching resulted in increased PKD1 activity, which gradually decreased during reformation (Fig. 2I; Fig. S2H). PKD1 activity in control conditions (silacz) was markedly reduced after 5 min and dropped back to basal levels after 10 min of adherens junction re-ligation. In contrast, p190RhoGAP-A depletion led to sustained activation of PKD1 during formation of adhesion complexes after 5 and 10 min (Fig. 2I). In summary, our data show PKD1 is a downstream target of RhoA and p190RhoGAP-A, regulating the formation and dissolution of adherens junctions by mediating phosphorylation of cortactin at S298.

Journal of Cell Science (2016) 129, 2416-2429 doi:10.1242/jcs.184721

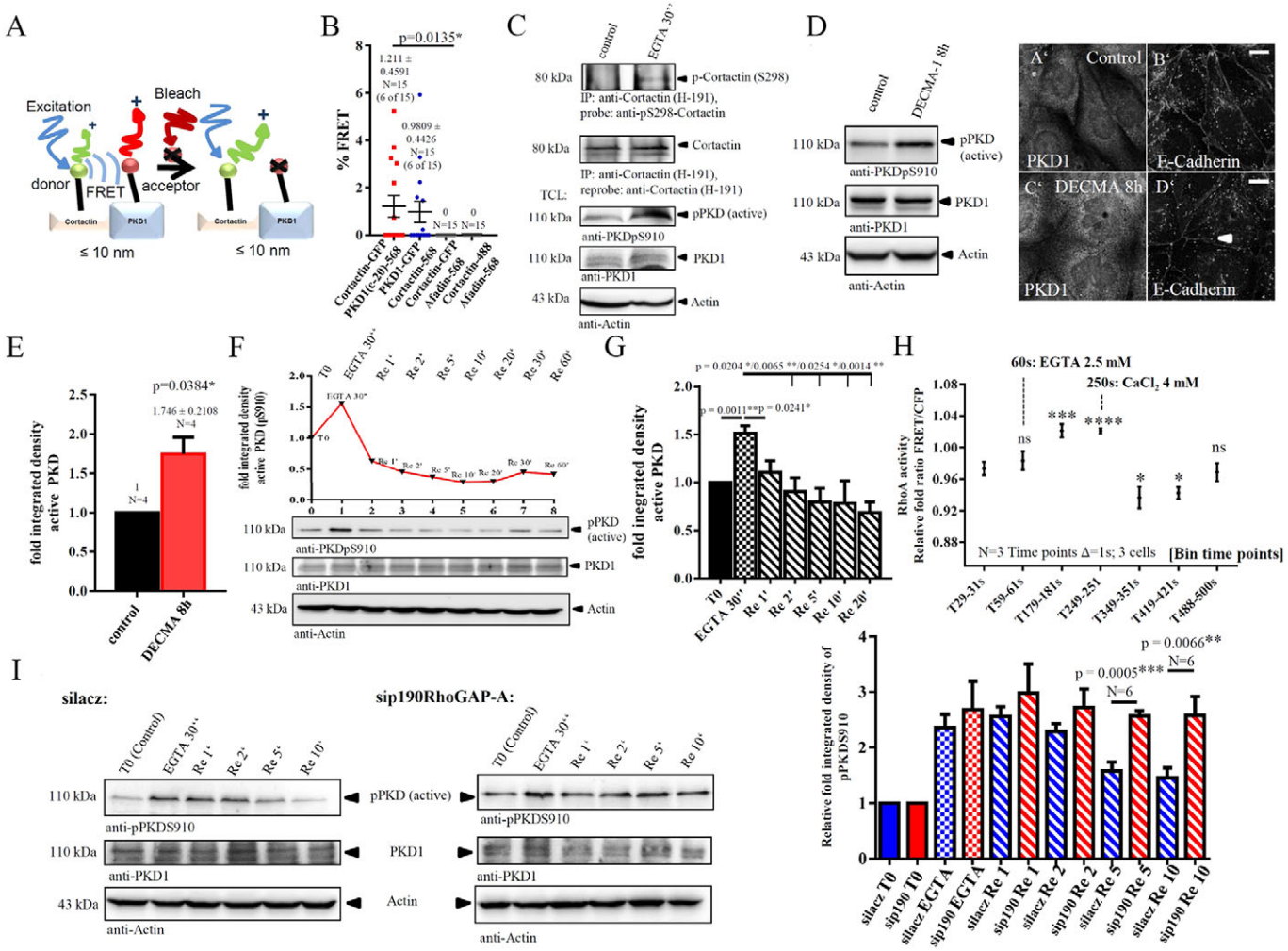

Fig. 2. PKD1 is activated by adherens junction breakdown and inactivated during assembly. (A) Schematic diagram of an AB-FRET experiment. (B) Quantitative AB-FRET analysis for the interaction of cortactin–GFP with endogenous PKD1 (clone C20 antibody) or Afadin (negative control) conjugated to Alexa Fluor 568 [PKD1(c-20)-568 and Afadin-568, respectively] as well as for PKD1–GFP with endogenous cortactin–Alexa-Fluor-568 or endogenous cortactin–Alexa-Fluor-488 and Afadin–Alexa-Fluor-568 (negative control) at Caco-2 adherens junctions. The graph shows the mean±s.e.m. percentage FRET (n=15 cells, three independent experiments). *P<0.05 (two-tailed unpaired Student's t-test). (C) Cortactin is phosphorylated at S298 after dissolution of adherens junctions with EGTA (4 mM, 30 s in growth media). Immunoprecipitation (IP) of endogenous cortactin from lysates of confluent Caco-2 cells. The immunoprecipitation probe was anti-cortactin-pS298 antibody, and the sample was reprobed with anti-cortactin antibody (H-191). One of three experiments is shown. Control lysates were probed for PKD activity, with anti-pS910 antibody. Loading controls were actin and PKD1. (D) PKD1 is activated by dissolution of adherens junctions with the E-cadherin blocking antibody DECMA-1 for 8 h. PKD1 activity is probed by anti-pS910 antibody in Caco-2 lysates. Loading controls were actin and PKD1. The images on the right-hand side show representative confocal sections of cells after DECMA-treatment with reduced E-cadherin staining at adherens junctions (arrowhead), recorded with similar settings. Scale bars: 10 µm. (E) Statistical analysis (means) of four experiments as shown in D. *P<0.05 (two-tailed paired Student's t-test). (F) PKD activation kinetics upon adherens junction dissolution and re-assembly in Caco-2 cells. Conditions were: untreated controls, 2 mM EGTA for 30 s (EGTA 30″), and 2 mM EGTA for 30 s and then re-addition of growth medium for the indicated time (Re, reformation). Blot panels show PKD activation kinetics detected by anti-PKD-pS910. One of five experiments is shown. (G) PKD activation from auto-phosphorylation blots of six experiments as indicated in F. Results are mean±s.e.m. (n=6). *P<0.05, **P<0.01 (two-tailed paired Student's t-test). (H) RhoA activity at adherens junctions detected using a RhoA-FRET-biosensor (Pertz et al., 2006). Dissolution of E-cadherin dimers was mediated by adding 2.5 mM EGTA to growth medium at 60 s (T60); reformation was mediated by adding 4 mM $CaCl_2$ at 250 s (T250). The graph shows the combined relative mean±s.e.m. FRET/CFP fluorescence ratio of the indicated binned time points from three experiments. *P<0.05; ***P<0.001; ****P<0.0001; ns, not significant (two-tailed unpaired Student's t-test in respect to T29–31). Inactive RhoA-T19N biosensor controls are shown in Fig. S3F. (I) p190RhoGAP-A and RhoA control PKD activity upon adherens junction formation and dissolution. Caco-2 cells were transfected with control siRNA against LacZ (silacz) or siRNA against p190RhoGAP-A (sip190RhoGAP-A). After 48 h silacz and sip190RhoGAP-A, samples were left untreated, stimulated with EGTA (2 mM for 30 s) or treated with EGTA followed by re-addition (Re) of growth medium. Left-hand side, PKD activation kinetics detected by anti-pPKDS910 for one of six independent experiments. Verification of p190RhoGAP-A knockdown is shown in Fig. S2H. Right-hand graph, relative mean±s.e.m. fold intensity of pPKDS910 signals in respect to controls. Blue bars, silacz control; red bars, sip190RhoGAP-A (sip190). **P<0.01; ***P<0.001 (two-tailed paired Student's t-test).

Role of cortactin as a major downstream target of PKD1 in adhesion complexes

Having established a RhoA–PKD1–cortactin pathway in adherens junctions, we next examined the role of cortactin and its S298 modification during assembly of the extended adhesion complex. First, we investigated whether phosphorylation of cortactin at S298 would alter its binding to E-cadherin (Helwani et al., 2004). Utilizing AB-FRET, we demonstrate that the E-cadherin–cortactin interaction was not significantly affected by the S298A mutant (Fig. 3A). Cortactin has also been shown to foster Arp-complex-

Journal of Cell Science

Journal of Cell Science (2016) 129, 2416-2429 doi:10.1242/jcs.184721

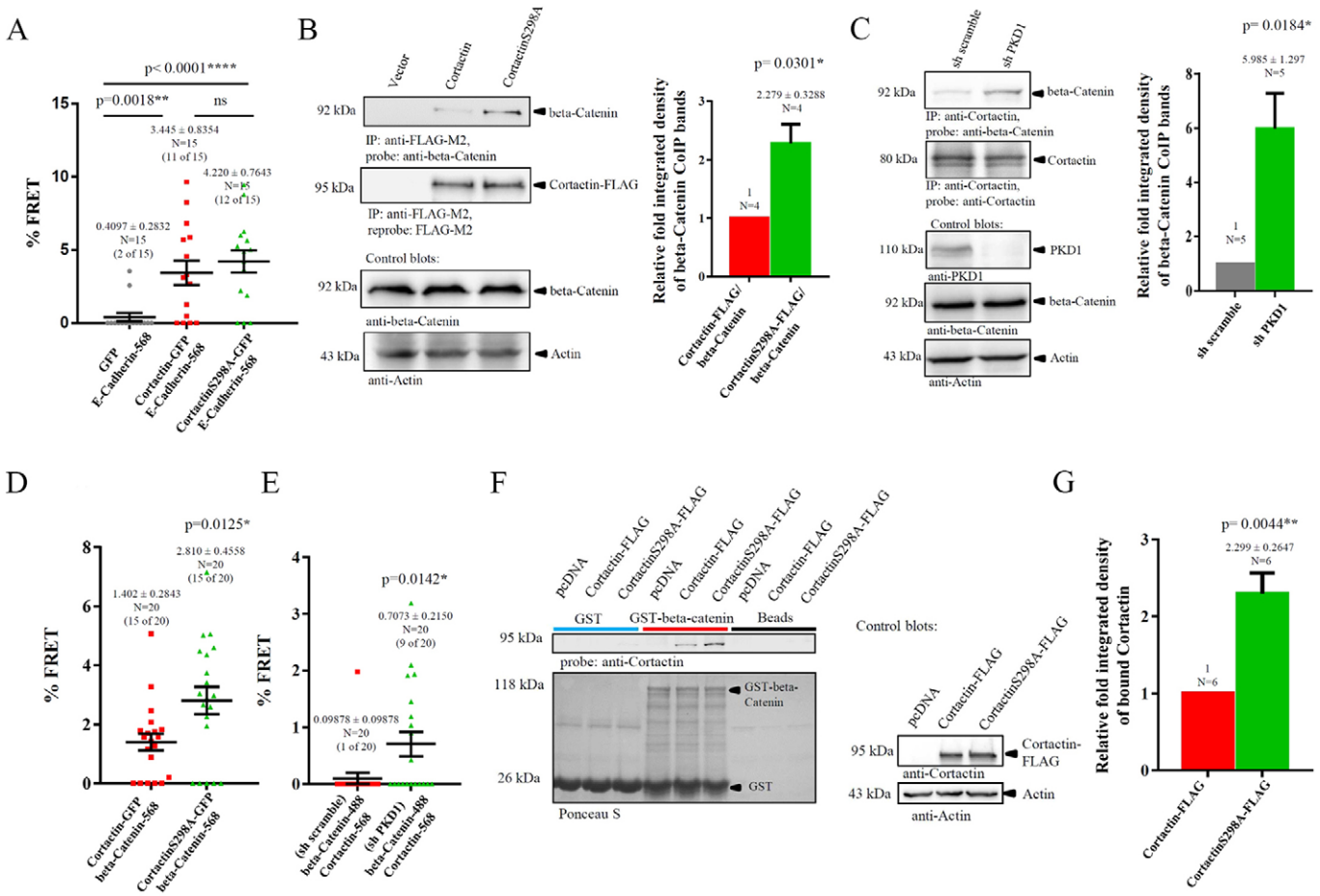

Fig. 3. Delineation of cortactin-dependent adhesion complex interactions. (A) Interaction of cortactin and cortactin-S298A with E-cadherin. Quantitative AB-FRET analysis of cortactin–GFP or cortactin-S298A–GFP with E-cadherin–Alexa-Fluor-568 (E-Cadherin-568) at Caco-2 adherens junctions. Negative control, GFP. The graph shows the mean±s.e.m. percentage FRET (n=15 cells and three independent experiments). **P<0.01; ***P<0.0001; ns, not significant (two-tailed unpaired Student's t-test). (B) Left-hand side, co-immunoprecipitation experiment (CoIP) of cortactin– and cortactin-S298A–FLAG expressed in confluent HEK293T cells with endogenous β-catenin. Cortactin–FLAG was immunoprecipitated (IP) by FLAG-M2 antibody. CoIP was performed with anti-β-catenin antibody, and reprobed with anti-cortactin antibody. Right-hand side, statistical analysis (mean±s.e.m.) of four CoIP experiments. *P<0.05 (two-tailed paired Student's t-test). (C) Interaction of endogenous cortactin with endogenous β-catenin following stable PKD1 depletion in HEK293T cells. Left-hand side, CoIP experiment of cortactin with β-catenin. Immunoprecipitation was performed with anti-cortactin antibody. CoIP was performed with anti-β-catenin antibody, and reprobed with anti-cortactin antibody. Right-hand side, statistical analysis (mean±s.e.m.) of five CoIP experiments. *P<0.05 (two-tailed paired Student's t-test). (D) Phosphorylation of cortactin at S298 modulates the direct interaction of cortactin with β-catenin. Quantitative AB-FRET analysis of cortactin–GFP or cortactin-S298A–GFP with endogenous β-catenin–Alexa-Fluor-568 (beta-Catenin-568) at Caco-2 adherens junctions. The graph shows the mean±s.e.m. percentage FRET (n=20 cells and three independent experiments). *P<0.05 (two-tailed unpaired Student's t-test). (E) Knockdown of PKD1 modulates the interaction of endogenous cortactin with endogenous β-catenin. Quantitative AB-FRET analysis for cortactin–Alexa-Fluor-488 (cortactin-488) with β-catenin–Alexa-Fluor-568 at adherens junctions in stable Caco-2 cells expressing scrambled shRNA (sh scramble) or shRNA against PKD1 (sh PKD1). Graph shows the mean±s.e.m. percentage FRET (n=20 cells and three independent experiments). *P<0.05 (two-tailed unpaired Student's t-test). Cell lines were as characterized in Fig. 1C. (F) Pulldown experiment to show binding of purified β-catenin–GST to FLAG-tagged cortactin or cortactin-S298 expressed in HEK293T cell lysates. Negative controls were empty beads and GST. The specificity control is pulldown of ENA-VSVG by β-catenin–GST (Fig. S3E). (G) Statistical analysis (mean±s.e.m.) of six pulldown experiments. **P<0.01 (two-tailed paired Student's t-test).

driven actin accumulation at adherens junctions (Helwani et al., 2004). We therefore investigated actin polymerization at adherens junctions by determining actin–GFP incorporation into filaments (Lorenz et al., 2004) utilizing FRET with phalloidin–Alexa-Fluor-568. In line with Helwani et al. (2004), ectopic expression of cortactin significantly increased actin polymerization and accumulation at adherens junctions, yet results for cortactin-S298A were not significantly different from those with wild-type cortactin (Fig. S3A,B). An evaluation of donor and acceptor pre-bleach intensities supported these findings, indicating a significant, phosphorylation-independent F-actin accumulation at adherens junctions of cortactin-transfected cells, whereas actin–GFP donor intensities were not significantly different (Fig. S3B). Thus, cortactin-S298-phosphorylation-dependent changes in cell–cell adhesion are not likely the result of altered junctional actin assembly.

We then asked whether binding of cortactin to E-cadherin would change linkage of the extended adhesion complex, that is, β-catenin to the E-cadherin intracellular domain. Interestingly, our AB-FRET data suggested that formation of β-catenin–E-cadherin complexes in the Caco-2 cortactin-knockdown cells was impaired (Fig. S3C). Given that E-cadherin and β-catenin bind with very high affinity, we investigated whether the number of E-cadherin–β-catenin complexes was reduced following cortactin depletion by additionally evaluating donor and acceptor pre-bleach intensities (Fig. S3D): β-catenin–GFP (donor) intensities were found to be

Journal of Cell Science (2016) 129, 2416-2429 doi:10.1242/jcs.184721

similar, whereas E-cadherin intensities were significantly reduced in the cortactin-knockdown samples, suggesting impaired complex formation. Thus, cortactin might foster E-cadherin adhesion complex formation, pointing to a putative molecular scaffold function in adherens junctions.

We therefore performed immunoprecipitation studies of cortactin and its S298A mutant to evaluate binding of endogenous β-catenin to cortactin in confluent HEK293T cells. β-Catenin co-precipitated with cortactin and binding was significantly enhanced when phosphorylation at S298 was prevented (Fig. 3B). Co-immunoprecipitation experiments of endogenous proteins upon knockdown of PKD1 (Fig. 3C) or co-expression of PKD1-CA and PKD1-KD (data not shown) yielded similar results. PKD1 depletion or PKD1-KD expression significantly increased binding of β-catenin (Fig. 3C). To test for a possible direct interaction of cortactin–GFP with β-catenin at adherens junctions we additionally performed FRET studies in Caco-2 cells. AB-FRET experiments revealed a direct interaction of both proteins, and this interaction was significantly enhanced when cortactin S298 phosphorylation was prevented (cortactin-S298A) (Fig. 3D). The interaction of endogenous β-catenin with cortactin was also significantly increased upon depletion of PKD1 (Fig. 3E). To support these findings, we performed GST-pulldown studies with bacterially purified β-catenin–GST. These experiments demonstrated a significantly increased interaction of cortactin-S298A–FLAG with β-catenin–GST in respect to wild-type cortactin (Fig. 3F,G). The F-actin-binding protein ENA-VSVG (Fig. S3E) was used as negative control to verify a specific interaction of β-catenin–GST and cortactin–FLAG proteins during pulldown experiments.

In summary our data suggest that phosphorylation of cortactin at S298 by PKD1 modifies its ability to interact with β-catenin in adhesion complexes.

Linkage of adhesion complexes to the actin cytoskeleton

E-cadherin adhesion complexes connect to the actin cytoskeleton for efficient cell–cell adhesion. Cortactin can directly bind F-actin (Weed et al., 2000; Wu and Parsons, 1993). Thus, cortactin could mediate a connection of E-cadherin to F-actin (Bershadsky, 2004; Helwani et al., 2004; Niessen et al., 2011). We therefore examined the direct binding of cortactin and its S298A mutant to phalloidin–Alexa-Fluor-568-labeled F-actin in adherens junctions. Interestingly, binding of cortactin to junctional F-actin was unaffected by the S298 phosphorylation. The classical actin-binding α-catenin and non-actin-binding β-catenin served as positive and negative controls, respectively (Fig. 4A). We therefore sought to identify whether additional molecules would act as F-actin linkers in the E-cadherin–β-catenin–cortactin adhesion complexes. A potential cytoskeletal linker is the actin-binding protein vinculin (Hazan et al., 1997; Peng et al., 2012). Vinculin can interact with β-catenin and α-catenin (Peng et al., 2010; Rimm et al., 1995; Yonemura et al., 2010). We performed co-immunoprecipitation studies with cortactin and its S298A mutant to evaluate binding of vinculin in HEK293T cells. Vinculin–GFP co-precipitated with cortactin–FLAG proteins and binding was significantly enhanced when phosphorylation at S298 was prevented (Fig. 4B). Co-immunoprecipitation experiments of endogenous vinculin and cortactin upon knockdown of PKD1 (Fig. 4C) or co-expression of PKD1-CA or PKD1-KD (data not shown) also returned similar results. Binding of endogenous vinculin to cortactin immunoprecipitates was significantly increased by PKD1 depletion (Fig. 4C) or PKD1-KD expression. To investigate a putative direct binding of vinculin–GFP to cortactin–FLAG proteins, we performed a quantitative AB-FRET analysis at Caco-2 adherens junctions (Fig. 4D). The interaction was significantly enhanced for the cortactin-S298A mutant (Fig. 4D). Knockdown of PKD1 likewise resulted in a significantly enhanced interaction of endogenous vinculin and cortactin (Fig. 4E). In all instances, donor and acceptor intensities were not significantly different for the tested conditions, demonstrating un-biased selection of cells during FRET studies (data not shown). To support FRET-based protein interaction studies, we again performed pulldown experiments utilizing His-tag-purified vinculin. In line with FRET assays, binding of cortactin-S298A–FLAG to vinculin–His_6 beads was significantly enhanced in respect to wild-type cortactin (Fig. 4F,G; Fig. S3F). E-cadherin–GFP was used as a control (Fig. S3F) to verify a specific interaction of vinculin–His_6 and cortactin–FLAG proteins during pulldown experiments.

Given that vinculin also binds to β-catenin (Peng et al., 2010), we examined whether cortactin was required for this interaction. We investigated the interaction of vinculin–GFP with endogenous β-catenin at Caco-2 adherens junctions by AB-FRET in cells expressing vector, cortactin–FLAG (dark, no dye) and cortactin-S298A–FLAG (dark, no dye) (Fig. 5A). Expression of the cortactin-S298A mutant significantly enhanced binding of vinculin to β-catenin, whereas wild-type cortactin had no significant effect. Depletion of PKD1 also significantly enhanced the interaction of endogenous β-catenin and vinculin (Fig. 5B). Again, evaluation of donor and acceptor intensities demonstrated un-biased selection of cells during experiments (data not shown). Enhanced vinculin–β-catenin interaction upon impaired cortactin-S298 phosphorylation was also shown by co-immunoprecipitation experiments with endogenous proteins upon co-expression of PKD1-CA and PKD1-KD (Fig. 5C). We next investigated whether β-catenin could bind to cortactin independently of its interaction with vinculin. Co-immunoprecipitation studies with knockdown of PKD1 and simultaneous knockdown of vinculin revealed that cortactin–β-catenin complexes were still able to form in the PKD1-knockdown samples, even if vinculin was depleted. Thus, enhanced binding of β-catenin to cortactin is possible without the facilitation of vinculin (Fig. S3G).

In the context of binding studies, we have additionally tested the interaction of cortactin with p120-catenin and α-catenin, which can bind β-catenin and vinculin (Fig. S3H). Interestingly, p120-catenin-co-immunoprecipitation with cortactin was also enhanced upon knockdown of PKD1 (Fig. S3H). This finding further supports the hypothesis that the p190-RhoGAP-A–RhoA pathway controls PKD1 activity, given that p120-catenin has been described to recruit p190-RhoGAP-A during adhesion formation (Wildenberg et al., 2006). By contrast, PKD1 depletion instead decreased co-precipitation of α-catenin in cortactin immunocomplexes, verifying the specificity of our binding studies (Fig. S3H).

To define the role of cortactin and its S298 phosphorylation in vinculin-mediated actin linkage, we examined F-actin binding of vinculin–GFP upon knockdown of PKD1 and following co-expression of cortactin in respective cells (Fig. 5D). The vinculin–GFP–F-actin interaction was significantly increased upon PKD1-depletion, with and without co-expression of wild-type cortactin (Fig. 5D), suggesting that cortactin–β-catenin–vinculin–F-actin complexes at adherens junctions are significantly impaired by cortactin S298 phosphorylation mediated by PKD1 (Fig. 5A–D).

Next, we wanted to verify complex linkage to E-cadherin. Endogenous E-cadherin was precipitated from PKD1-depleted cells or controls, and co-precipitated endogenous β-catenin, cortactin and

Journal of Cell Science (2016) 129, 2416-2429 doi:10.1242/jcs.184721

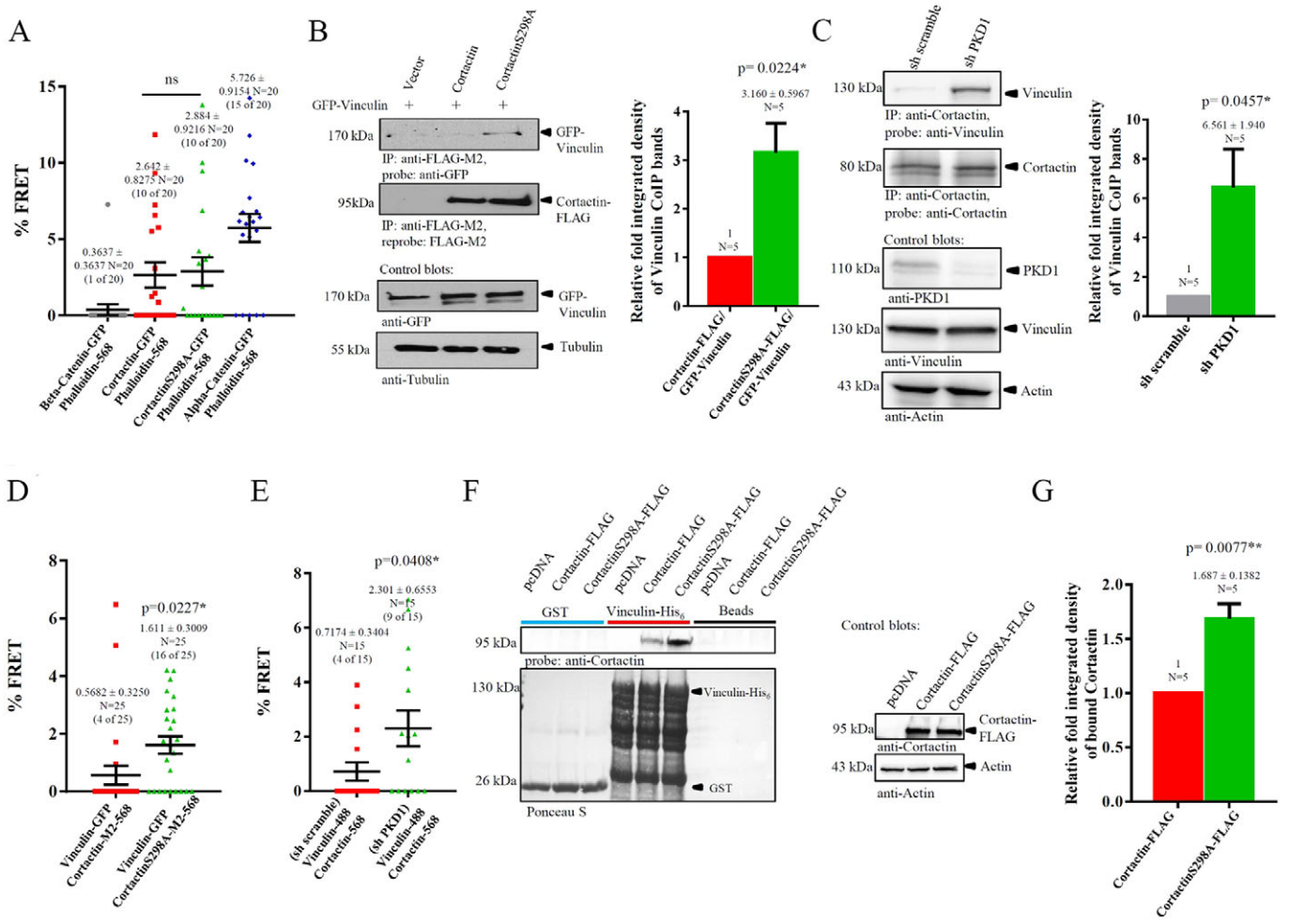

Fig. 4. Connection of E-cadherin adhesion complexes to the actin cytoskeleton. (A) Binding of cortactin to the actin cytoskeleton at adherens junctions. Quantitative AB-FRET analysis for cortactin–GFP or cortactin-S298A–GFP with F-actin (phalloidin–Alexa-Fluor-568; phallodin-568) at Caco-2 adherens junctions. Negative control was β-catenin–GFP; positive control was α-catenin–GFP. The graph shows the mean±s.e.m. percentage FRET (*n*=20 cells and four independent experiments). ns, not significant (two-tailed unpaired Student's *t*-test). (B) Left-hand side, CoIP experiment of cortactin– and cortactin-S298A–FLAG with vinculin–GFP expressed in HEK293T cells. Immunoprecipitation (IP) of cortactin–FLAG was achieved with FLAG-M2-antibody. CoIP was performed with anti-GFP antibody, and reprobed with anti-cortactin antibody. Right-hand side, statistical analysis (mean±s.e.m.) of five independent CoIP experiments. **P*<0.05 (two-tailed paired Student's *t*-test). (C) Interaction of endogenous cortactin with endogenous vinculin following stable depletion of PKD1 in HEK293T cells. Left-hand side, CoIP experiment of cortactin with vinculin. Immunoprecipitation was achieved with anti-cortactin antibody. CoIP was performed with anti-vinculin antibody, and reprobed with anti-cortactin antibody. Right-hand side, statistical analysis (mean±s.e.m.) of five CoIP experiments. **P*<0.05 (two-tailed paired Student's *t*-test). (D) Phosphorylation of cortactin at S298 modulates the direct interaction of cortactin with vinculin. Quantitative AB-FRET analysis for vinculin–GFP with cortactin or cortactin-S298A bound to FLAG-M2–Alexa-Fluor-568 (-M2-568) at Caco-2 adherens junctions. The graph shows the mean±s.e.m. percentage FRET (*n*=25 cells and three independent experiments). **P*<0.05 (two-tailed unpaired Student's *t*-test). (E) Knockdown of PKD1 modulates the interaction of endogenous cortactin with endogenous vinculin. Quantitative AB-FRET analysis for vinculin–Alexa-Fluor-488 (vinculin-488) with cortactin–Alexa-Fluor-568 (cortactin-568) at adherens junctions in stable Caco-2 cells expressing scrambled shRNA (sh scramble) or shRNA against PKD1 (sh PKD1). The graph shows the mean±s.e.m. percentage FRET (*n*=15 cells and three independent experiments). Cell lines were as characterized in Fig. 1C. **P*<0.05 (two-tailed unpaired Student's *t*-test). (F) Pulldown experiment to show binding of purified vinculin–His_6 to cortactin– or cortactin-S298–FLAG in lysates from HEK293T cells. Negative controls were empty beads and GST. The specificity control is pulldown of E-cadherin–GFP by vinculin–His_6 (Fig. S3F). (G) Statistical analysis (mean±s.e.m.) of five pulldown experiments. ***P*<0.01 (two-tailed paired Student's *t*-test).

vinculin were detected (Fig. 5E–H; Fig. S4A). Again, significantly more β-catenin, cortactin and vinculin were found in E-cadherin immunocomplexes upon knockdown of PKD1 (Fig. 5E–H; Fig. S4A). Thus, phosphorylation of cortactin at S298 by PKD1 seems to impair linkage of E-cadherin–β-catenin–cortactin–vinculin complexes to the actin cytoskeleton.

Vinculin mediates changes in cell–cell adhesion triggered by PKD1-induced phosphorylation of cortactin

The data shown above suggest that vinculin might help to mediate changes in cell–cell adhesion triggered by PKD1-induced phosphorylation of cortactin. We therefore depleted vinculin in Caco-2 cells stably expressing GFP, cortactin–GFP or cortactin-S298A–GFP, respectively. These cells were used for hanging-droplet cell–cell adhesion assays that were quantified according to Ehrlich et al., 2002 (Fig. 6A,B; Fig. S4B). In line with previous experiments, cortactin-S298A–GFP cells expressing scrambled shRNA formed significantly larger clusters (>50 cells, 52.2%) compared to cells expressing cortactin–GFP (28.3%) or GFP (20%). Knockdown of vinculin significantly reduced cell–cell adhesion in all samples, but the S298A mutant cells were more prominently affected (only

Journal of Cell Science (2016) 129, 2416-2429 doi:10.1242/jcs.184721

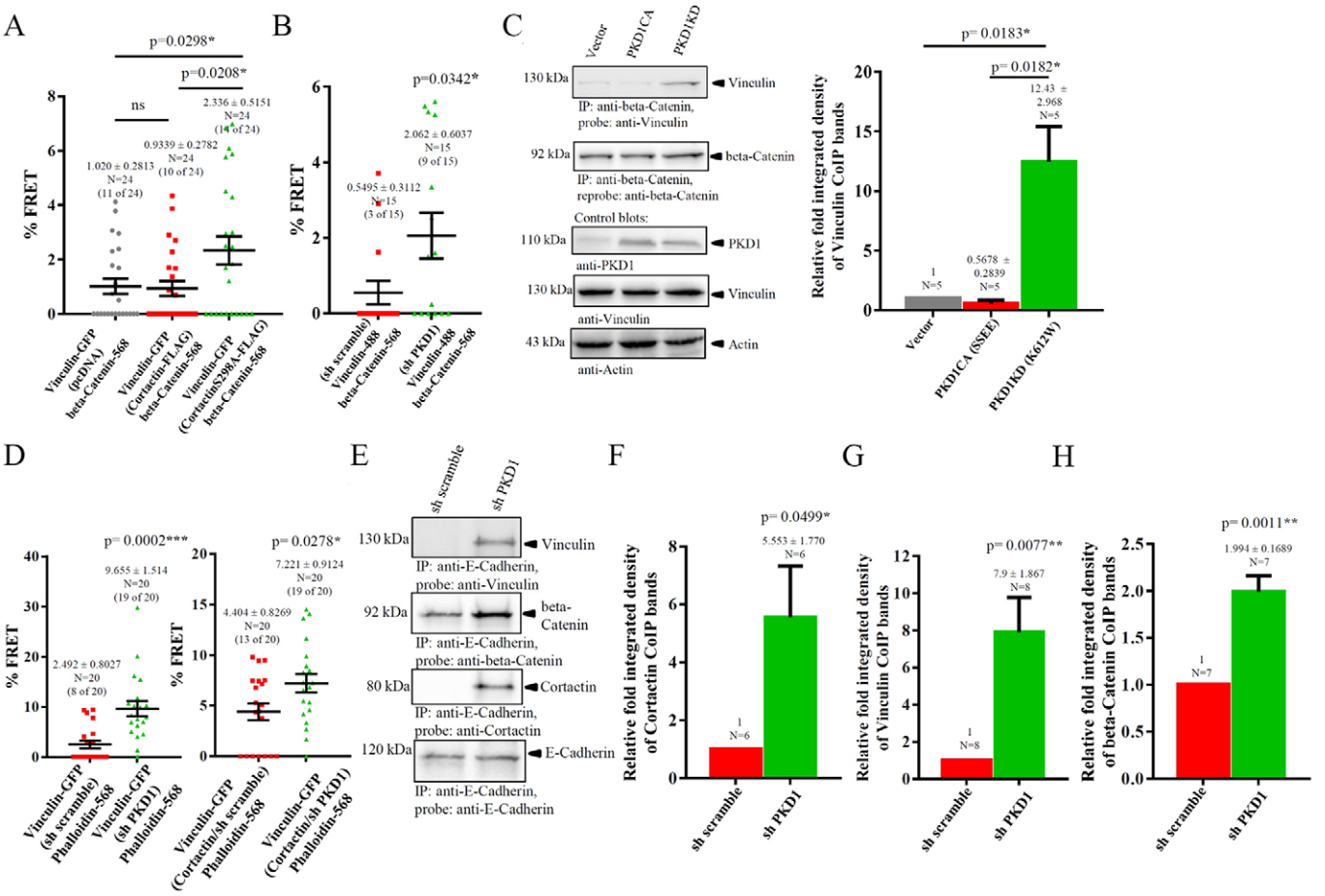

Fig. 5. Interaction of vinculin with β-catenin and complex cytoskeleton linkage. (A) Quantitative AB-FRET analysis for vinculin–GFP and endogenous β-catenin–Alexa-Fluor-568 (beta-Catenin-568) at Caco-2 adherens junctions. Cells were additionally transfected with vector, cortactin–FLAG (dark) or cortactin-S298A–FLAG (dark). The graph shows the mean±s.e.m. percentage FRET (n=24 cells and three independent experiments). *P<0.05; ns, not significant (two-tailed unpaired Student's t-test). (B) Knockdown of PKD1 modulates the interaction of endogenous vinculin with endogenous β-catenin. Quantitative AB-FRET analysis for vinculin–Alexa-Fluor-488 (vinculin-488) with β-catenin–Alexa-Fluor-568 at adherens junctions in Caco-2 cells expressing scrambled shRNA (sh scramble) or shRNA against PKD1 (sh PKD1). The graph shows the mean±s.e.m. percentage FRET (n=15 cells and three independent experiments). *P<0.05 (two-tailed unpaired Student's t-test). Cell lines were as characterized in Fig. 1C. (C) Interaction of endogenous β-catenin with endogenous vinculin following co-expression of vector, PKD1-CA and PKD1-KD in HEK293T cells. Left-hand side, CoIP experiment of β-catenin with vinculin. Immunoprecipitation (IP) was achieved with anti-β-catenin antibody. CoIP was performed with anti-vinculin, and reprobed with anti-β-catenin antibody. Right-hand side, statistical analysis (mean±s.e.m.) of five CoIP experiments. *P<0.05 (two-tailed paired Student's t-test). (D) Phosphorylation of cortactin modulates the interaction of vinculin with the actin cytoskeleton. Quantitative AB-FRET analysis for the interaction of vinculin–GFP with F-actin (phalloidin–Alexa-Fluor-568; phalloidin-568) at adherens junctions in stable sh scramble and sh PKD1 Caco-2 cells or stable cells additionally transfected with cortactin–FLAG (dark). The graph shows the mean±s.e.m. percentage FRET (n=20 cells and four independent experiments). *P<0.05; ***P<0.0001 (two-tailed unpaired Student's t-test). (E) Linkage of adhesion complexes with β-catenin, cortactin and vinculin to E-cadherin upon stable depletion of PKD1 in HEK293T cells. Representative CoIP experiment. Immunoprecipitation was performed with anti-E-cadherin antibody. CoIPs was performed with anti-β-catenin, anti-cortactin or anti-vinculin antibodies, and reprobed with anti-E-cadherin antibody. (F–H) Statistical analysis (mean±s.e.m.) of six cortactin CoIPs (F), eight vinculin CoIPs (G) and seven β-catenin CoIPs (H). *P<0.05; ***P<0.0001 (two-tailed paired Student's t-test).

2.1% of clusters had more than 50 cells, 38.2% of clusters had between 11 and 50 cells, and 59.7% had aggregates consisting of 1–10 cells). In comparison to cortactin–GFP, the number of single cells and small aggregates (1–10 cells) was significantly increased from 51.6% (cortactin–GFP) to 59.7% for the cortactin-S298A–GFP samples (Fig. 6A,B). Thus, upon knockdown of vinculin, cortactin-S298A mutant cells almost completely lost their ability to form large aggregates, whereas cortactin–GFP samples in comparison formed midsize and comparatively more larger clusters (>50 cells) (Fig. 6B; Table S1). In summary, these data suggest that vinculin is indeed required for the dynamic modulation of cell–cell adhesion by PKD1 and cortactin during formation of adherens junctions.

PKD1 controls cortactin-S298-phosphorylation-dependent protein interactions in mouse colonic epithelia

To substantiate our findings in a relevant *in vivo* situation, we investigated whether the molecular interactions depending on the phosphorylation of cortactin by PKD1 could also be demonstrated in non-transformed colonic epithelia of mice. To this end, we employed a transgenic mouse line with doxycycline-inducible overexpression of wild-type PKD1. Mice were treated with doxycycline for 30 days. Histological specimens of the intestine were stained with an anti-PKD1 antibody to verify induction or overexpression of PKD1 (Fig. 7A). In addition, we probed PKD auto-phosphorylation (pS916) and activation loop phosphorylation (pS744 and S748) in samples to demonstrate enhanced activity of

Journal of Cell Science (2016) 129, 2416-2429 doi:10.1242/jcs.184721

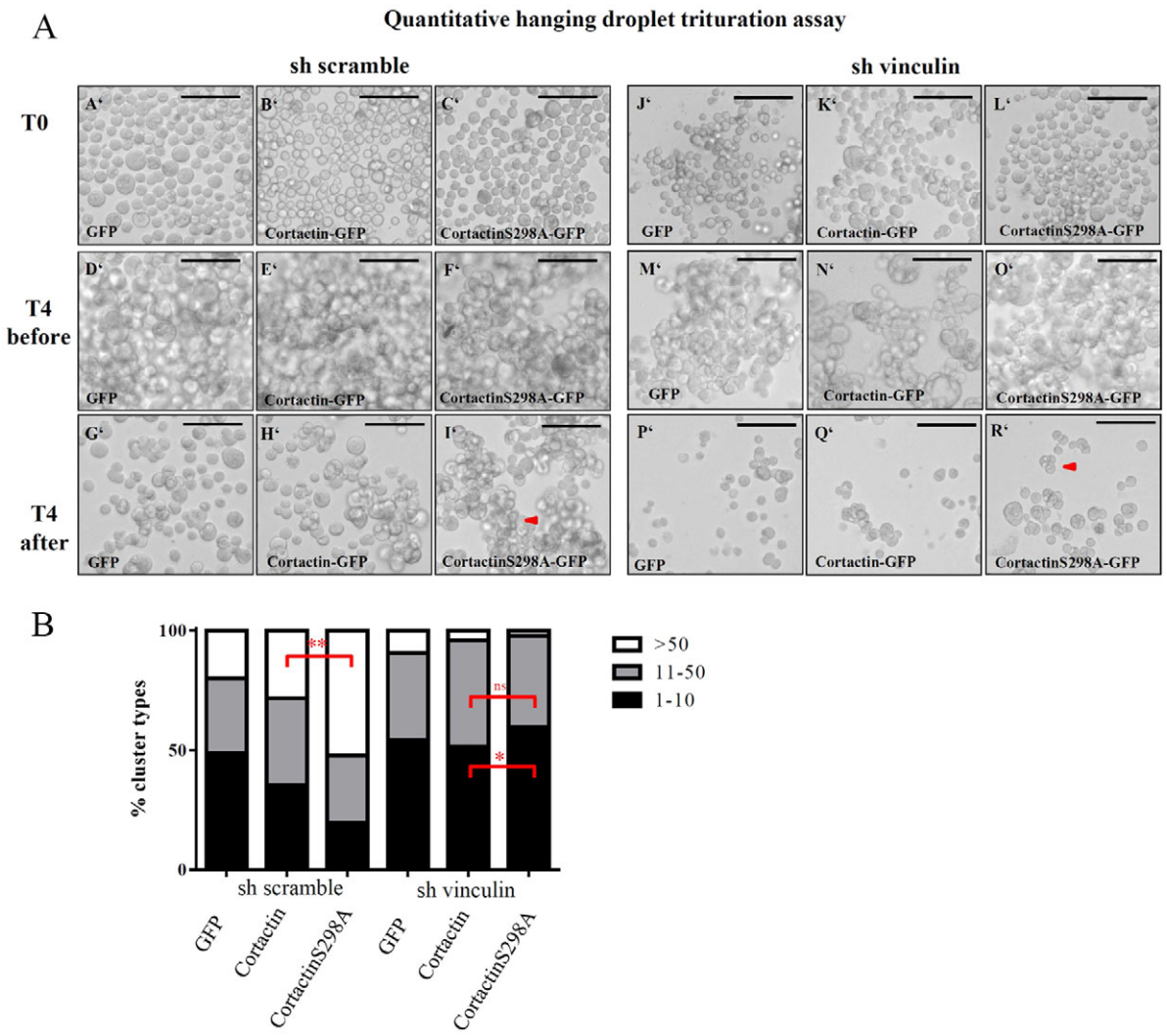

Fig. 6. Vinculin mediates changes in cell–cell adhesion triggered by PKD1-induced phosphorylation of cortactin. (A) Quantitative hanging droplet cell–cell adhesion assay. Stable Caco-2 cells expressing GFP, cortactin–GFP and cortactin-S298A–GFP were depleted of vinculin (sh vinculin). Sh scramble, non-specific control. Images were taken after 4 h of adhesion (10,000 cells per droplet) at 10× magnification before and after trituration. Representative magnified images are depicted. Scales bar: 100 µm. Arrowheads mark clusters. (B) Quantitative analysis of cell–cell adhesion assays from A. The graph shows a statistical analysis of the percentage of cluster types for 1–10, 11–50 and aggregates of >50 cells. Three assays with two images per condition were analyzed (>1000 cells/image). **P*<0.05; ***P*<0.01; ns, not significant (two-tailed unpaired Student's *t*-test). A complete quantitative analysis is presented in Table S4. Cortactin–GFP and cortacin-S298A–GFP transgene expression, and knockdown of vinculin is shown in Fig. S4B.

PKD1 upon ectopic expression (Fig. S4C). A morphometric analysis of histological specimens stained with E-cadherin, β-catenin and DAPI indicated enhanced proliferation in crypts, as demonstrated by a significantly increased total cell number per crypt, crypt depth and crypt circumference in the colon of PKD1 knock-in mice, in line with previous data (Sinnett-Smith et al., 2011) (Fig. 7B–D, Fig. S4D). The evaluation of marker proteins in colon lysates demonstrated that E-cadherin, β-catenin and cortactin expression levels were not visibly altered and vinculin expression appeared slightly diminished in PKD1 knock-in (PKD-KI) samples (Fig. S4E). In addition, histological sections were stained with antibodies against claudin 1, E-cadherin, β-catenin, cortactin and vinculin to evaluate putative changes in the localized expression of adherens junction and tight junction proteins. Our quantitative data, obtained from adherens junctions of three mice each, indicated that claudin1, E-cadherin and β-catenin expression levels were not altered to a significant extent in PKD1-KI mice, whereas junctional cortactin and vinculin levels were reduced by 11.1 and 12.7%, respectively (Fig. S4F). We also did not see significant changes in intestinal permeability *in vivo* upon addition of FITC–dextran to the drinking water of the respective mice (Fig. S4G). Nevertheless, even though wild-type PKD1 did not seem to affect tight junctions, we investigated putative effects on E-cadherin mediated cell–cell adhesion *in vivo*.

To evaluate protein–protein interactions for cortactin and β-catenin, as well as cortactin and vinculin, we performed an AB-FRET analysis of colon sections (Fig. 7A). Our data verify an interaction of cortactin with β-catenin (Fig. 7E, representative images are shown in Fig. S4H) and of cortactin with vinculin (Fig. 7F). The mean percentage FRET was significantly reduced in PKD1-overexpressing mice by 57.3% for cortactin and β-catenin, and 50.9% for cortactin and vinculin, respectively. Although, we cannot exclude effects due to slightly reduced cortactin and vinculin expression, changes in percentage FRET values by far exceed reduced protein levels for cortactin and vinculin at adherens junctions, which amount to ∼10%, and might also be attributed to

Journal of Cell Science (2016) 129, 2416-2429 doi:10.1242/jcs.184721

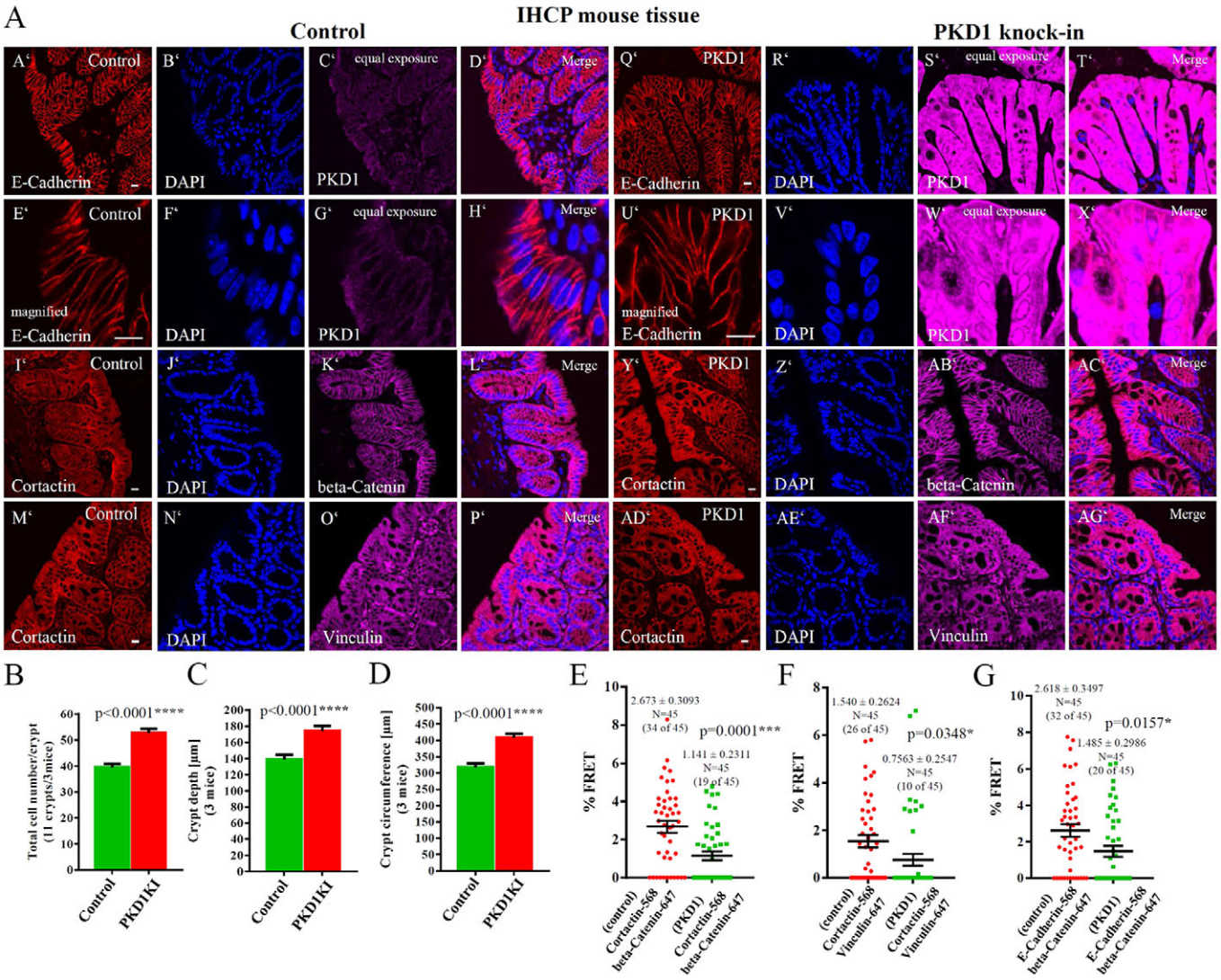

Fig. 7. Cortactin-phosphorylation-dependent protein interactions in colon epithelia of PKD1 transgenic mice. (A) PKD1 transgenic knock-in and control mice treated with doxycycline for 30 days. Panels A′–H′ and Q′–X′, show the immunohistochemistry of colon sections (anti-PKD1 anti-E-cadherin antibody). Images were acquired with a confocal microscope with similar settings and are single confocal sections. Panels I′–L′ and Y′–AC′, show immunohistochemistry with anti-cortactin and anti-β-catenin antibodies. Panels M′–P′ and AD′–AG′ show immunohistochemistry with anti-cortactin and anti-vinculin antibodies. Nuclei are stained with DAPI. Scale bars: 10 µm. (B–D) Morphometric analysis of control and PKD1-KI mice. Immunohistochemistry was performed with DAPI, anti-β-catenin and anti-E-cadherin antibody. Images were taken at 10× magnification with a Keyence BZ-9000 microscope (example images are shown in Fig. S4D). Three mice each (11 crypts/mouse) were quantified (mean±s.e.m.). ***P<0.0001 (two-tailed unpaired Student's t-test). (B) The total number of cells/crypt. (C) Crypt depth (µm) measured from spatially calibrated images. (D) Crypt circumference (µm) measured from spatially calibrated images. (E) Expression of PKD1 modulates the interaction of endogenous cortactin and β-catenin in colonic epithelia of mice. Quantitative AB-FRET analysis of cortactin–Alexa-Fluor-568 (cortactin-568) and β-catenin–Alexa-Fluor-647 (beta-Catenin-647) at adherens junctions of colonic epithelia. The graph shows the mean±s.e.m. percentage FRET (n=45 cells and three mice). Representative FRET images are shown in Fig. S4H. (F) Expression of PKD1 modulates the interaction of endogenous cortactin and vinculin in colonic epithelia. Quantitative AB-FRET analysis for the interaction of cortactin–Alexa-Fluor-568 and vinculin–Alexa-Fluor-647 (vinculin-647) at adherens junctions of colonic epithelia. The graph shows the mean±s.e.m. percentage FRET (n=45 cells and three mice). (G) Expression of PKD1 impairs E-cadherin–β-catenin complex formation at adherens junctions of colon epithelia. Quantitative AB-FRET analysis for E-cadherin–Alexa-Fluor-568 (E-Cadherin-568) with β-catenin–Alexa-Fluor-647 at adherens junctions of colon epithelia. The graph shows the mean±s.e.m. percentage FRET (n=45 cells and three mice). *P<0.05; ***P<0.001 (two-tailed unpaired Student's t-test).

impaired complex formation. As an indirect measure for the extent of cell–cell adhesions, we further evaluated the interaction of β-catenin with E-cadherin in the respective sections. The mean percentage FRET in PKD1-KI animals was reduced by 43.3% (Fig. 7G), suggesting significantly impaired formation of β-catenin–E-cadherin-complexes, and compromised formation, but not a full ablation, of cell–cell adhesion complexes *in vivo*.

Our data therefore identify several new protein interactions implicated in the formation of E-cadherin-based adherens junctions that are also detectable in non-transformed cells of colon epithelia from mice. Our data further suggest that presence of cortactin and its posttranslational modification by PKD1 are likely to play an important role in epithelial cell–cell adhesion not only *in vitro* but also *in vivo*.

DISCUSSION

Dynamic changes in cell–cell adhesion junctions are, to a large extent, associated with the formation or dissolution of adhesive

Journal of Cell Science (2016) 129, 2416-2429 doi:10.1242/jcs.184721

contact zones that govern morphogenetic processes during development, wound healing or cancer metastasis (Takeichi, 2011, 2014). We here delineate a pathway that is initiated with the ligation or dissolution of E-cadherin adhesion contacts and transduced by the modulation of RhoA activity through p190RhoGAP-A (Noren et al., 2003) to PKD1 (Fig. 2A–I). PKD1 in-turn phosphorylates the adhesion-resident protein cortactin (Eiseler et al., 2010), which alters adhesion complex composition. A major part of this study was to elucidate how the presence of cortactin and its phosphorylation by PKD1 alters protein–protein interactions in the E-cadherin adhesion complex and consequently the linkage of E-cadherin cell–cell contacts to the actin cytoskeleton (Figs 3, 4 and 5). Cortactin has been previously described to associate with E-cadherin (Helwani et al., 2004; Ren et al., 2009) and p120-catenin (Boguslavsky et al., 2007). Here, we were able to establish two new protein interactions in the E-cadherin adhesion complex: binding of cortactin to β-catenin and vinculin. Literature further suggests that cortactin enhances actin polymerization and/or accumulation at adherens junctions (Helwani et al., 2004). We were able to verify that this was indeed the case. Although we have previously shown that cortactin affects Arp-dependent synergistic actin polymerization at the leading edge through its PKD1-mediated phosphorylation at S298 (Eiseler et al., 2010), polymerization of junctional actin was independent of the S298 phosphorylation (Fig. S3A,B). Thus, changes in junctional actin polymerization are unlikely to be responsible for the PKD1-controlled cell–cell adhesion phenotypes mediated through cortactin. We rather show that cortactin acts as a molecular scaffold that exhibits phosphorylation-dependent interactions with β-catenin and vinculin. These interactions are significantly enhanced when cortactin is not phosphorylated by PKD1 (Figs 3B–G and 4B–G). In addition, we demonstrate that PKD1-dependent phosphorylation of cortactin modulates the interaction of β-catenin with vinculin, and of vinculin with the actin cytoskeleton (Fig. 5A–D). In both cases, non-phosphorylated cortactin strongly supports the interaction. Complexes are also fully linked to E-cadherin and this is enhanced upon PKD1 depletion (Fig. 5E–H). Thus, cortactin and PKD1 play a crucial role for the integration of vinculin-associated protein interactions in the E-cadherin adhesion complex during formation of adherens junctions. Knockdown of vinculin therefore strongly impairs enhanced cell–cell adhesion conferred by the non-phosphorylatable cortactin mutant (Fig. 6A,B). By recapitulating interactions in non-transformed colon epithelia of mice, we add additional emphasis to our findings (Fig. 7E–G). Previously, cortactin deficiency in mice had been demonstrated to affect mammalian zygotic development by modulating its association with actin filaments (Yu et al., 2010), but a role in cell–cell adhesion in mice had not been investigated. Different studies have attributed cortactin a role in epithelial (Rezaee et al., 2013; Zhao et al., 2012) and endothelial barrier functions (Dudek et al., 2004; Schnoor et al., 2011). However, wild-type PKD1-KI mice, in line with literature (Sinnett-Smith et al., 2011), did not display obvious physical phenotypes or alterations in tight junction proteins, such as claudin 1 (Fig. S4F,G). Our molecular interaction studies with E-cadherin and β-catenin (Fig. 7G) suggest that cell–cell adhesion is significantly impaired in PKD1-KI animals, but not completely abrogated. Thus, it is likely that tight junctions are still able to form, and putative impairments in barrier function were not severe enough to cause clear physiological or histological dysfunctions under basal conditions.

In summary, our data indicate that cortactin, unexpectedly, is a crucial molecular scaffold in the E-cadherin adhesion complex during formation of adherens junctions, altering cell–cell adhesion by modulating β-catenin- and vinculin-mediated protein interaction in a manner dependent on PKD1 phosphorylation (Fig. 8).

MATERIALS AND METHODS

Cell culture, plasmids, antibodies and dye reagents

HEK293T cells (from the ATCC) were maintained in Dulbecco's modified Eagle's medium [DMEM; with 10% fetal calf serum (FCS) and penicillin-streptomycin] and transfected using PEI (Polysciences Inc.). Caco-2 cells (from the DSMZ, German collection of microorganisms and cell cultures) were cultivated in MEM medium (GlutaMAX, with 20% FCS, non-essential amino acids, penicillin-streptomycin) and transfected using Lipofectamine LTX (Invitrogen, Darmstadt, Germany) for cDNA vectors or Oligofectamine (Invitrogen, Darmstadt, Germany) for small interfering RNAs (siRNAs). Stable Caco-2 cells expressing GFP, cortactin–GFP and cortactin-S298A–GFP were generated by G418 selection (6 mg/ml) for 2 months and sorted to establish polyclonal lines. Stable Caco-2 cells with knockdown of cortactin and PKD1 or non-specific shRNA scramble cell lines were generated by lentiviral transduction followed by selection with puromycin (6 µg/ml) for 3 weeks. Lentiviruses were generated as described previously (Eiseler et al., 2012). To generate stable Caco-2 cells expressing GFP, cortactin–GFP and cortactin-S298A–GFP with shRNA scramble or vinculin shRNAs, stable cells were transduced with respective lentiviruses and subjected to selection with G418 and puromycin (6 mg/ml, 6 µg/ml) for 3 weeks. All experiments with stable cell lines were conducted after 2 weeks of growth in standard growth medium to allow for recovery from the selection. A full list of cDNA expression plasmids, lentiviral shRNA constructs and siRNAs is provided in Table S1. A full list of antibodies with dilutions used in this study is available in Table S2.

Total cell lysates and co-immunoprecipitation

Total cell lysates and co-immunoprecipitation experiments (CoIPs) were performed as described previously (Eiseler et al., 2010, 2012). CoIPs were performed in transiently transfected or stable HEK293T cells. Following western blot transfer, quantitative analysis was performed by measuring integrated band density using ImageJ. Integrated density of CoIPs was normalized to precipitated bait protein. Quantified PKD1-pS910 signals in cell lysates were normalized to PKD1 expression. Values shown represent fold change with respect to controls.

Protein purification and pulldown experiments

β-Catenin–GST and vinculin–His_6 were expressed in BL21-bacteria and purified as described previously (Eiseler et al., 2016). For pulldown experiments, 20 µl of purified protein on beads was incubated for 4 h with 2 mg of total cell lysate from HEK293T cells expressing the indicated binding partners. Pulldown assays were performed as described previously (Eiseler et al., 2016). Empty beads and GST-conjugated protein beads were used as negative controls.

F-actin-binding studies

F-actin cosedimentation experiments with cell lysates were performed as described previously (Eiseler et al., 2007). For cosedimentation experiments 50 µg of 100,000 ***g*** lysate was incubated with 20 µg *in vitro* polymerized F-actin (AKL-99, Cytoskeleton Inc.). Cosedimentation was assessed following ultracentrifugation at 100,000 ***g*** for 1 h at room temperature by loading equal amounts of supernatant and pellet fractions for SDS-PAGE and detection on western blots.

Preparation of mouse colon sections from mice and IHC-staining

Inducible PKD1-(Tet-ON)-mice and C57BL/6×129 control mice were maintained in a pathogen-free environment. Mice were generated by injecting the p2Lox targeting vector (Iacovino et al., 2011) with PKD1-cDNA in A2lox.Cre-ES-cells and subsequent implantation in pseudo-pregnant host animals. Mice were maintained with food and drinking water available *ad libitum*. PKD1-expression was induced by the administration of doxycycline (1 g/l and 10 g/l sucrose) to the drinking water of 12-week-old

Journal of Cell Science (2016) 129, 2416-2429 doi:10.1242/jcs.184721

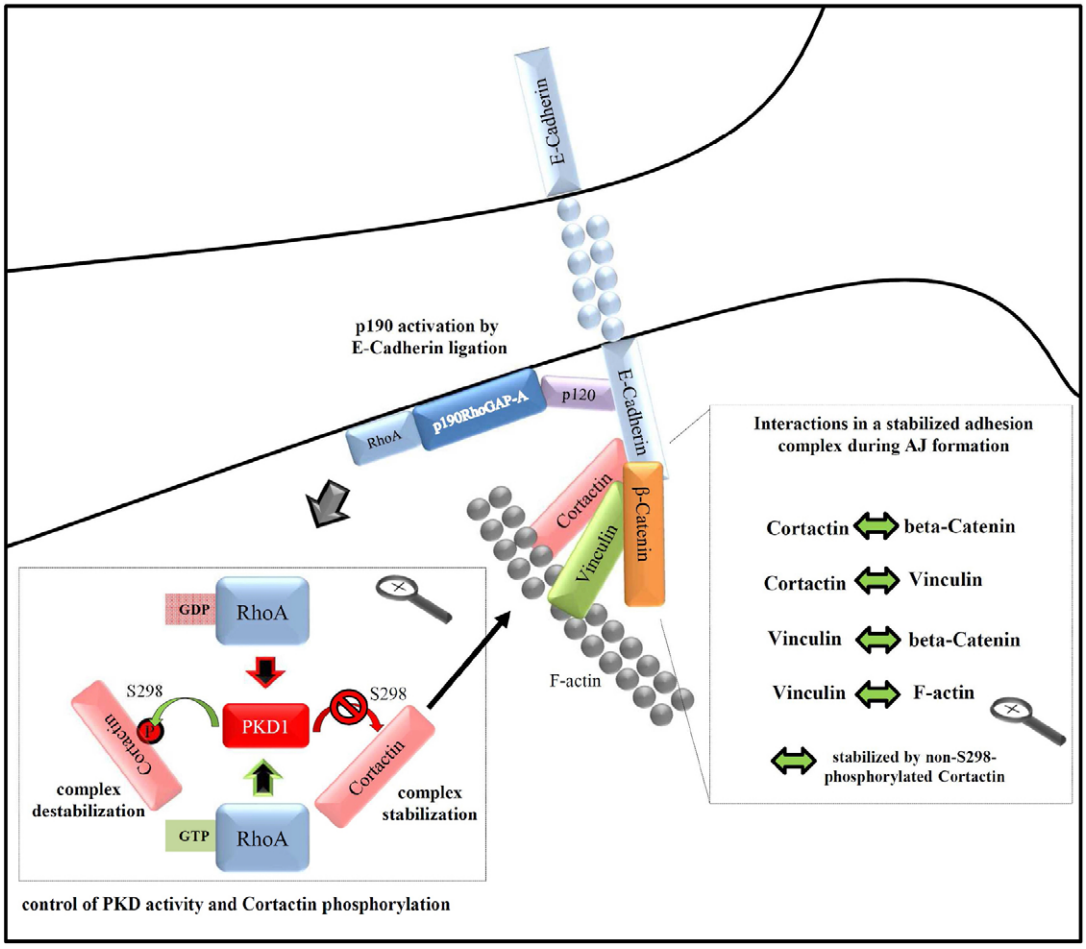

Fig. 8. Regulation of cell-cell adhesion by cortactin and PKD1 during ligation of adherens junctions. Ligation of E-cadherin results in the activation of p190RhoGAP-A which locally inactivates RhoA. Inactivation of RhoA impairs PKD activity and cortactin-S298 phosphorylation as well as 14-3-3β-binding (Eiseler et al., 2010) (overview-box, left-hand side). Cortactin that is not phosphorylated at S298 substanitally enhances or stabilizes β-catenin- and vinculin-mediated proteins interactions during adherens junction formation (overview-box, right-hand side).

male mice for 30 days. Control mice were also treated with doxycycline and animals were killed according to animal welfare regulations (state government of Baden Wuerttemberg, proposal no: 1169). The colon was removed, flushed with PBS, fixed and embedded in paraffin. Sections (5 µm) were treated and stained as described previously (Armacki et al., 2014; Wille et al., 2014). Primary antibodies were detected by Alexa-Fluor-568- and -647-conjugated secondary antibodies; nuclei were stained with DAPI. Confocal images sections were acquired using a Leica TCS SP8-HCS microscope using a 40× oil immersion objective.

Intestinal permeability assay

FITC-dextran (6 mg/10 g bodyweight, Sigma-Aldrich, catalog number: FD4) was administered to mice by oral gavage after starvation overnight. 4 h after administration, mice were killed and serum was collected. The concentration of FITC–dextran in the serum was determined with a microplate reader [excitation of 485 nm, emission of 528 nm (bandpasses were 20 nm)].

Immunofluorescence confocal microscopy and acceptor-photobleach FRET

Immunofluorescence and AB-FRET staining was performed as described previously (Eiseler et al., 2012). Experiments were analyzed by confocal laser scanning microscopes LSM710 (Zeiss, Jena, Germany) and TCS SP8-HCS (Leica, Mannheim, Germany) equipped with 40×, 63× Plan Apo oil or water immersion objectives. Images were acquired in sequential scan mode. Gain and offset were set in a way that all cellular structures were imaged within the linear range of detectors having no saturated pixels and black-level background values.

AB-FRET experiments were performed with transiently transfected or stable Caco-2 cells, fixed, processed and stained as stated previously (Eiseler et al., 2012; Wille et al., 2014). This method allows the determination of protein–protein interactions indicated by an apparent molecular proximity below 10 nm (Eiseler et al., 2012, 2016; Gu et al., 2004; Kunkel and Newton, 2009; Oser et al., 2010; Valente et al., 2012; Wille et al., 2014; Wouters et al., 1998; Zeug et al., 2012). The FRET acceptor in a region of interest (ROI) was bleached by an intensive laser line and increase in donor fluorescence, indicating FRET, was measured. AB-FRET measurements were carried out by acquiring pre- and post-bleach images of donor and acceptor using an automated time series. Donor dyes in cells were either GFP-tagged proteins or Alexa-Fluor-488-labeled antibodies. Acceptors were labeled with Alexa-Fluor-568 antibodies or phalloidin–Alexa-Fluor-568 (F-actin). Owing to auto-fluorescence, proteins in mouse samples were probed with Alexa-Fluor-568 (donor) and Alexa-Fluor-647 (acceptor) antibodies. As an internal threshold, 8-bit images (256 gray values) were used for recording raw data to only register substantial changes in fluorescence intensities as respective gray value changes. FRET experiments were acquired from at least three independent transfections or sources. Cells were randomly sampled from slides. In experiments with ectopic transgenes, cells with very strong ectopic expression were not recorded to avoid artifacts. Image analysis was performed using ImageJ. Quantitative FRET analysis was executed by calculating the mean

percentage FRET and s.e.m. for each cell from non-thresholded raw data for six Sub-ROIs randomly placed on the linear adhesion junctions of Caco-2 cells within the bleached region [%FRET=(($Donor_{post}$−$Donor_{pre}$)/$Donor_{post}$)×100]. Cells that failed to show FRET in the bleach-region were set to zero during analysis. Results are presented as scatter graphs with single percentage FRET values. Numbers on top of graphs indicate mean percentage FRET values and s.e.m. for all cells evaluated. Numbers in brackets indicate the number of cells with FRET in the bleach-region. FRET calculations from raw data sorted by the figure they are shown in are in Table S3.

FRET-ratio-live imaging with Caco-2 cells

A RhoA-FRET-FLARE sensor (Pertz et al., 2006) was used to quantify activation of RhoA at adherens junctions. RhoA activity was measured by simultaneous ratio live imaging of CFP (470–500 nm) and FRET signals (525–550 nm) using a LSM710 or Leica TCS SP8-HCS confocal microscope (37°C, 5% CO_2) with 90% open pinholes following excitation of the donor (CFP) with a continuous 405 nm laser line at low intensities in ROI scanning mode (LSM710) (Δ=1 s). A RhoA-T19N-FLARE sensor was used as a negative control.

Hanging droplet cell–cell adhesion assays

Qualitative hanging droplet cell–cell adhesion assays were performed by seeding 6000 or 10,000 transiently transfected or stable cells from three independent sources in 20 µl droplets of growth medium on the inner lid of a 10-cm dish (at least six replicas/condition). Hanging droplets were incubated for 24 h on dishes filled with PBS to create a humidified atmosphere in cell culture incubators. After 24 h, aggregates were triturated by a 20-times re-suspension with a 10-µl pipette. Clusters were documented at 10× magnification using a Keyence BZ-8000 bright field microscope. Quantitative hanging droplet cell–cell adhesion assays were performed by seeding 10,000 cells in hanging droplets. Cell aggregates were documented at 10× magnification pre- and post-trituration (20×10 µl) after 4 h. Post-trituration aggregates were quantified by determining the number of aggregates and respective cell numbers, with clusters of 1–10, 11–50 and >50 cells. Results are presented as percentage cluster types in respect to the total cell number of images (Ehrlich et al., 2002).

Cell–cell adhesion on E-cadherin–Fc surfaces

E-cadherin–Fc surfaces were generated and utilized to measure cell adhesion as described previously (Drees et al., 2005b). In brief, glass cover slips coated with streptavidin were labeled with biotin–Protein-A and functionalized with a human E-cadherin–Fc (IgG1) fragment affinity purified from serum-free cell culture supernatant of transfected HEK293T cells. Cell adhesion assays with stable Caco-2 cells on E-cadherin–Fc surfaces were performed by incubating 2000 cells in 20-µl droplets (two replicas per condition and three slides) for 2 h and 4 h in a humidified atmosphere in a cell culture incubator. Cover slips were washed three times by the addition and aspiration of PBS followed by fixation with formaldehyde and mounting onto microscopy slides. Cell adhesion to E-cadherin–Fc surfaces was quantified by acquiring stitched images of the entire droplet areas at 4× magnification using a Keyence BZ-9000 microscope and counting of adhered cells.

Statistical analyses

Statistical analysis was performed using Prism software version 6.00 for Windows (GraphPad Software, San Diego, CA). Graphs depict mean±s.e.m. for all conditions. Statistical significance is indicated by asterisks (ns, not significant; *P<0.05 to 0.01; **P=0.01 to 0.001; ***P<0.001; ****P<0.0001).

Acknowledgements

The authors want to acknowledge use of the Imaging Core Facility for 'Multiphoton and Confocal Microscopy' at Ulm University. We thank Ralf Kemkemer, J. W. Nelson and Keith Burridge for providing valuable research reagents. We thank Susanne Fluhr for excellent technical assistance and Professor Starzinski-Powitz for critical reading and reagents.

Competing interests

The authors declare no competing or financial interests.

Author contributions

T.E. conceived the study. T.E. and T.S. supervised experiments. R.S., S.-F.K. and T.E. performed experiments. R.S., T.E. and T.S. evcaluated data. M.R.S. generated the PKD1 knock-in mice. J.V.L. produced and verified the pCortactinS298 antibody and provided valuable intellectual input. A.K. provided PKD1 knockin-mice for the study. T.E. and T.S. wrote the manuscript, and share senior authorship.

Funding

This work was funded by the Deutsche Forschungsgemeinschaft (DFG) [grant numbers EI792/3-1 to T.E., SE 676/10-1 to T.S., CRC 1149 project A6]. Work in the J.V.L. laboratory is supported by Fonds Wetenschappelijk Onderzoek (FWO – Fund for Scientific Research Flanders); and by the EU Seventh Framework Programme (FP7) [grant number 259770 'Lungtarget'].

Supplementary information

Supplementary information available online at
http://jcs.biologists.org/lookup/doi/10.1242/jcs.184721.supplemental

References

Aberle, H., Schwartz, H., Hoschuetzky, H. and Kemler, R. (1996). Single amino acid substitutions in proteins of the armadillo gene family abolish their binding to alpha-catenin. *J. Biol. Chem.* **271**, 1520-1526.

Aitken, A. (2006). 14-3-3 proteins: a historic overview. *Semin. Cancer Biol.* **16**, 162-172.

Armacki, M., Joodi, G., Nimmagadda, S. C., de Kimpe, L., Pusapati, G. V., Vandoninck, S., Van Lint, J., Illing, A. and Seufferlein, T. (2014). A novel splice variant of calcium and integrin-binding protein 1 mediates protein kinase D2-stimulated tumour growth by regulating angiogenesis. *Oncogene* **33**, 1167-1180.

Bardella, C., Costa, B., Maggiora, P., Patane, S., Olivero, M., Ranzani, G. N., De Bortoli, M., Comoglio, P. M. and Di Renzo, M. F. (2004). Truncated RON tyrosine kinase drives tumor cell progression and abrogates cell-cell adhesion through E-cadherin transcriptional repression. *Cancer Res.* **64**, 5154-5161.

Benjamin, J. M., Kwiatkowski, A. V., Yang, C., Korobova, F., Pokutta, S., Svitkina, T., Weis, W. I. and Nelson, W. J. (2010). AlphaE-catenin regulates actin dynamics independently of cadherin-mediated cell-cell adhesion. *J. Cell Biol.* **189**, 339-352.

Bershadsky, A. (2004). Magic touch: how does cell-cell adhesion trigger actin assembly? *Trends Cell Biol.* **14**, 589-593.

Boguslavsky, S., Grosheva, I., Landau, E., Shtutman, M., Cohen, M., Arnold, K., Feinstein, E., Geiger, B. and Bershadsky, A. (2007). p120 catenin regulates lamellipodial dynamics and cell adhesion in cooperation with cortactin. *Proc. Natl. Acad. Sci. USA* **104**, 10882-10887.

Buckley, C. D., Tan, J., Anderson, K. L., Hanein, D., Volkmann, N., Weis, W. I., Nelson, W. J. and Dunn, A. R. (2014). The minimal cadherin-catenin complex binds to actin filaments under force. *Science* **346**, 1254211.

Davis, M. A., Ireton, R. C. and Reynolds, A. B. (2003). A core function for p120-catenin in cadherin turnover. *J. Cell Biol.* **163**, 525-534.

Drees, F., Pokutta, S., Yamada, S., Nelson, W. J. and Weis, W. I. (2005a). Alpha-catenin is a molecular switch that binds E-cadherin-beta-catenin and regulates actin-filament assembly. *Cell* **123**, 903-915.

Drees, F., Reilein, A. and Nelson, W. J. (2005b). Cell-adhesion assays: fabrication of an E-cadherin substratum and isolation of lateral and Basal membrane patches. *Methods Mol. Biol.* **294**, 303-320.

Dudek, S. M., Jacobson, J. R., Chiang, E. T., Birukov, K. G., Wang, P., Zhan, X. and Garcia, J. G. N. (2004). Pulmonary endothelial cell barrier enhancement by sphingosine 1-phosphate: roles for cortactin and myosin light chain kinase. *J. Biol. Chem.* **279**, 24692-24700.

Ehrlich, J. S., Hansen, M. D. H. and Nelson, W. J. (2002). Spatio-temporal regulation of Rac1 localization and lamellipodia dynamics during epithelial cell-cell adhesion. *Dev. Cell* **3**, 259-270.

Eiseler, T., Schmid, M. A., Topbas, F., Pfizenmaier, K. and Hausser, A. (2007). PKD is recruited to sites of actin remodelling at the leading edge and negatively regulates cell migration. *FEBS Lett.* **581**, 4279-4287.

Eiseler, T., Döppler, H., Yan, I. K., Kitatani, K., Mizuno, K. and Storz, P. (2009). Protein kinase D1 regulates cofilin-mediated F-actin reorganization and cell motility through slingshot. *Nat. Cell Biol.* **11**, 545-556.

Eiseler, T., Hausser, A., De Kimpe, L., Van Lint, J. and Pfizenmaier, K. (2010). Protein kinase D controls actin polymerization and cell motility through phosphorylation of cortactin. *J. Biol. Chem.* **285**, 18672-18683.

Eiseler, T., Kohler, C., Nimmagadda, S. C., Jamali, A., Funk, N., Joodi, G., Storz, P. and Seufferlein, T. (2012). Protein kinase D1 mediates anchorage-dependent and -independent growth of tumor cells via the zinc finger transcription factor Snail1. *J. Biol. Chem.* **287**, 32367-32380.

Eiseler, T., Wille, C., Koehler, C., Illing, A. and Seufferlein, T. (2016). Protein kinase D2 assembles a multiprotein complex at the Trans-Golgi network to regulate matrix metalloproteinase secretion. *J. Biol. Chem.* **291**, 462-477.
Ferl, R. J., Manak, M. S. and Reyes, M. F. (2002). The 14-3-3s. *Genome Biol.* **3**, REVIEWS3010.
Gu, Y., Di, W. L., Kelsell, D. P. and Zicha, D. (2004). Quantitative fluorescence resonance energy transfer (FRET) measurement with acceptor photobleaching and spectral unmixing. *J. Microsc.* **215**, 162-173.
Han, S. P., Gambin, Y., Gomez, G. A., Verma, S., Giles, N., Michael, M., Wu, S. K., Guo, Z., Johnston, W., Sierecki, E. et al. (2014). Cortactin scaffolds Arp2/3 and WAVE2 at the epithelial zonula adherens. *J. Biol. Chem.* **289**, 7764-7775.
Hartsock, A. and Nelson, W. J. (2008). Adherens and tight junctions: structure, function and connections to the actin cytoskeleton. *Biochim. Biophys. Acta* **1778**, 660-669.
Hazan, R. B., Kang, L., Roe, S., Borgen, P. I. and Rimm, D. L. (1997). Vinculin is associated with the E-cadherin adhesion complex. *J. Biol. Chem.* **272**, 32448-32453.
Helwani, F. M., Kovacs, E. M., Paterson, A. D., Verma, S., Ali, R. G., Fanning, A. S., Weed, S. A. and Yap, A. S. (2004). Cortactin is necessary for E-cadherin-mediated contact formation and actin reorganization. *J. Cell Biol.* **164**, 899-910.
Huber, A. H. and Weis, W. I. (2001). The structure of the beta-catenin/E-cadherin complex and the molecular basis of diverse ligand recognition by beta-catenin. *Cell* **105**, 391-402.
Iacovino, M., Bosnakovski, D., Fey, H., Rux, D., Bajwa, G., Mahen, E., Mitanoska, A., Xu, Z. and Kyba, M. (2011). Inducible cassette exchange: a rapid and efficient system enabling conditional gene expression in embryonic stem and primary cells. *Stem Cells* **29**, 1580-1588.
Ireton, R. C., Davis, M. A., van Hengel, J., Mariner, D. J., Barnes, K., Thoreson, M. A., Anastasiadis, P. Z., Matrisian, L., Bundy, L. M., Sealy, L. et al. (2002). A novel role for p120 catenin in E-cadherin function. *J. Cell Biol.* **159**, 465-476.
Janssens, K., De Kimpe, L., Balsamo, M., Vandoninck, S., Vandenheede, J. R., Gertler, F. and Van Lint, J. (2009). Characterization of EVL-I as a protein kinase D substrate. *Cell Signal.* **21**, 282-292.
Kunkel, M. T. and Newton, A. C. (2009). Spatiotemporal dynamics of kinase signaling visualized by targeted reporters. *Curr. Protoc. Chem. Biol.* **1**, 17-18.
Lorch, J. H., Klessner, J., Park, J. K., Getsios, S., Wu, Y. L., Stack, M. S. and Green, K. J. (2004). Epidermal growth factor receptor inhibition promotes desmosome assembly and strengthens intercellular adhesion in squamous cell carcinoma cells. *J. Biol. Chem.* **279**, 37191-37200.
Lorenz, M., DesMarais, V., Macaluso, F., Singer, R. H. and Condeelis, J. (2004). Measurement of barbed ends, actin polymerization, and motility in live carcinoma cells after growth factor stimulation. *Cell Motil. Cytoskeleton* **57**, 207-217.
Mackintosh, C. (2004). Dynamic interactions between 14–3–3 proteins and phosphoproteins regulate diverse cellular processes. *Biochem. J.* **381**, 329-342.
Niessen, C. M., Leckband, D. and Yap, A. S. (2011). Tissue organization by cadherin adhesion molecules: dynamic molecular and cellular mechanisms of morphogenetic regulation. *Physiol. Rev.* **91**, 691-731.
Noren, N. K., Arthur, W. T. and Burridge, K. (2003). Cadherin engagement inhibits RhoA via p190RhoGAP. *J. Biol. Chem.* **278**, 13615-13618.
Oser, M., Mader, C. C., Gil-Henn, H., Magalhaes, M., Bravo-Cordero, J. J., Koleske, A. J. and Condeelis, J. (2010). Specific tyrosine phosphorylation sites on cortactin regulate Nck1-dependent actin polymerization in invadopodia. *J. Cell Sci.* **123**, 3662-3673.
Peng, X., Cuff, L. E., Lawton, C. D. and DeMali, K. A. (2010). Vinculin regulates cell-surface E-cadherin expression by binding to beta-catenin. *J. Cell Sci.* **123**, 567-577.
Peng, X., Maiers, J. L., Choudhury, D., Craig, S. W. and DeMali, K. A. (2012). alpha-Catenin uses a novel mechanism to activate vinculin. *J. Biol. Chem.* **287**, 7728-7737.
Pertz, O., Hodgson, L., Klemke, R. L. and Hahn, K. M. (2006). Spatiotemporal dynamics of RhoA activity in migrating cells. *Nature* **440**, 1069-1072.
Pokutta, S., Drees, F., Yamada, S., Nelson, W. J. and Weis, W. I. (2008). Biochemical and structural analysis of alpha-catenin in cell-cell contacts. *Biochem. Soc. Trans.* **36**, 141-147.
Provost, E. and Rimm, D. L. (1999). Controversies at the cytoplasmic face of the cadherin-based adhesion complex. *Curr. Opin. Cell Biol.* **11**, 567-572.
Ren, G., Helwani, F. M., Verma, S., McLachlan, R. W., Weed, S. A. and Yap, A. S. (2009). Cortactin is a functional target of E-cadherin-activated Src family kinases in MCF7 epithelial monolayers. *J. Biol. Chem.* **284**, 18913-18922.
Rezaee, F., DeSando, S. A., Ivanov, A. I., Chapman, T. J., Knowlden, S. A., Beck, L. A. and Georas, S. N. (2013). Sustained protein kinase D activation mediates respiratory syncytial virus-induced airway barrier disruption. *J. Virol.* **87**, 11088-11095.
Rimm, D. L. and Morrow, J. S. (1994). Molecular cloning of human E-cadherin suggests a novel subdivision of the cadherin superfamily. *Biochem. Biophys. Res. Commun.* **200**, 1754-1761.
Rimm, D. L., Koslov, E. R., Kebriaei, P., Cianci, C. D. and Morrow, J. S. (1995). Alpha 1(E)-catenin is an actin-binding and -bundling protein mediating the attachment of F-actin to the membrane adhesion complex. *Proc. Natl. Acad. Sci. USA* **92**, 8813-8817.
Schneider, M. R. and Kolligs, F. T. (2015). E-cadherin's role in development, tissue homeostasis and disease: insights from mouse models: tissue-specific inactivation of the adhesion protein E-cadherin in mice reveals its functions in health and disease. *Bioessays* **37**, 294-304.
Schnoor, M., Lai, F. P. L., Zarbock, A., Kläver, R., Polaschegg, C., Schulte, D., Weich, H. A., Oelkers, J. M., Rottner, K. and Vestweber, D. (2011). Cortactin deficiency is associated with reduced neutrophil recruitment but increased vascular permeability in vivo. *J. Exp. Med.* **208**, 1721-1735.
Shibamoto, S., Hayakawa, M., Takeuchi, K., Hori, T., Oku, N., Miyazawa, K., Kitamura, N., Takeichi, M. and Ito, F. (1994). Tyrosine phosphorylation of beta-catenin and plakoglobin enhanced by hepatocyte growth factor and epidermal growth factor in human carcinoma cells. *Cell Adhes. Commun.* **1**, 295-305.
Sinnett-Smith, J., Rozengurt, N., Kui, R., Huang, C. and Rozengurt, E. (2011). Protein kinase D1 mediates stimulation of DNA synthesis and proliferation in intestinal epithelial IEC-18 cells and in mouse intestinal crypts. *J. Biol. Chem.* **286**, 511-520.
Sundram, V., Chauhan, S. C., Ebeling, M. and Jaggi, M. (2012). Curcumin attenuates beta-catenin signaling in prostate cancer cells through activation of protein kinase D1. *PLoS ONE* **7**, e35368.
Takeichi, M. (2011). Self-organization of animal tissues: cadherin-mediated processes. *Dev. Cell* **21**, 24-26.
Takeichi, M. (2014). Dynamic contacts: rearranging adherens junctions to drive epithelial remodelling. *Nat. Rev. Mol. Cell Biol.* **15**, 397-410.
Takeichi, M., Watabe, M., Shibamoto, S. and Ito, F. (1994). Cadherin-dependent organization and disorganization of epithelial architecture. *Princess Takamatsu Symp.* **24**, 28-37.
Valente, C., Turacchio, G., Mariggio, S., Pagliuso, A., Gaibisso, R., Di Tullio, G., Santoro, M., Formiggini, F., Spano, S., Piccini, D. et al. (2012). A 14–3–3gamma dimer-based scaffold bridges CtBP1-S/BARS to PI(4)KIIIbeta to regulate post-Golgi carrier formation. *Nat. Cell Biol.* **14**, 343-354.
Weed, S. A., Karginov, A. V., Schafer, D. A., Weaver, A. M., Kinley, A. W., Cooper, J. A. and Parsons, J. T. (2000). Cortactin localization to sites of actin assembly in lamellipodia requires interactions with F-actin and the Arp2/3 complex. *J. Cell Biol.* **151**, 29-40.
Weis, W. I. and Nelson, W. J. (2006). Re-solving the cadherin-catenin-actin conundrum. *J. Biol. Chem.* **281**, 35593-35597.
Wildenberg, G. A., Dohn, M. R., Carnahan, R. H., Davis, M. A., Lobdell, N. A., Settleman, J. and Reynolds, A. B. (2006). p120-catenin and p190RhoGAP regulate cell-cell adhesion by coordinating antagonism between Rac and Rho. *Cell* **127**, 1027-1039.
Wille, C., Kohler, C., Armacki, M., Jamali, A., Gossele, U., Pfizenmaier, K., Seufferlein, T. and Eiseler, T. (2014). Protein kinase D2 induces invasion of pancreatic cancer cells by regulating matrix metalloproteinases. *Mol. Biol. Cell* **25**, 324-336.
Wouters, F. S., Bastiaens, P. I. H., Wirtz, K. W. A. and Jovin, T. M. (1998). FRET microscopy demonstrates molecular association of non-specific lipid transfer protein (nsL-TP) with fatty acid oxidation enzymes in peroxisomes. *EMBO J.* **17**, 7179-7189.
Wu, H. and Parsons, J. T. (1993). Cortactin, an 80/85-kilodalton pp60src substrate, is a filamentous actin-binding protein enriched in the cell cortex. *J. Cell Biol.* **120**, 1417-1426.
Yamada, S., Pokutta, S., Drees, F., Weis, W. I. and Nelson, W. J. (2005). Deconstructing the cadherin-catenin-actin complex. *Cell* **123**, 889-901.
Yonemura, S., Wada, Y., Watanabe, T., Nagafuchi, A. and Shibata, M. (2010). alpha-Catenin as a tension transducer that induces adherens junction development. *Nat. Cell Biol.* **12**, 533-542.
Yu, D., Zhang, H., Blanpied, T. A., Smith, E. and Zhan, X. (2010). Cortactin is implicated in murine zygotic development. *Exp. Cell Res.* **316**, 848-858.
Zeug, A., Woehler, A., Neher, E. and Ponimaskin, E. G. (2012). Quantitative intensity-based FRET approaches–a comparative snapshot. *Biophys. J.* **103**, 1821-1827.
Zhao, J., Wei, J., Mialki, R., Zou, C., Mallampalli, R. K. and Zhao, Y. (2012). Extracellular signal-regulated kinase (ERK) regulates cortactin ubiquitination and degradation in lung epithelial cells. *J. Biol. Chem.* **287**, 19105-19114.